Development of discontinuous Galerkin methods for time-domain electromagnetics

Stéphane Lanteri

INRIA Sophia Antipolis-Méditerranée
NACHOS project-team
Stephane.Lanteri@irnia.fr

2nd CNPq-INRIA workshop - HOSCAR project
LNCC, Petropolis, Brazil
September 10-13, 2012

Scientific objectives

Design, analysis and validation of numerical methods and high performance resolution algorithms for the computer simulation of wave propagation problems in complex domains and heterogeneous media

Research directions

- Systems of linear PDEs with variable coefficients
  - Discretization
    - Discontinuous finite element (DG) methods on unstructured meshes
    - High order polynomial interpolation
    - *p*-, *h*- and *hp*-adaptivity
    - Numerical treatment of complex propagation media models
  - Resolution
    - Accurate and efficient time integration strategies
    - Domain decomposition (DD) methods
  - High peformance computing
    - Algorithmic aspects and parallel programming paradigms
    - Implementation issues for large-scale 3D simulations

Computational electromagnetics

- System of Maxwell equations
- Dispersive propagation media
- Applications involve the interaction of electromagnetic waves with,
  1. biological tissues (biocem),
  2. geological media (georadar).

James Clerk Maxwell (1831-1879)

Computational geoseismics

- System of elastodynamic equations
- Viscoelastic propagation media
- Applications deal with the propagation of seismic waves,
  1. generated by an explosive source (earthquake dynamics),
  2. in the subsurface (resource prospection).

History

- Created in July 2007
- Common project-team with J.A. Dieudonné (JAD) Mathematics Laboratory UMR CNRS 6621, University of Nice-Sophia Antipolis (UNSA)

Permanent staff

- INRIA
  - Loula Fezoui [DR2]
  - Stéphane Lanteri [DR2]
- JAD Laboratory, UNSA
  - Stéphane Descombes [PR]
  - Victorita Dolean [MdC]
- INRIA/UNSA Chair
  - Claire Scheid [MdC]

Content

Discontinuous Galerkin Time Domain method

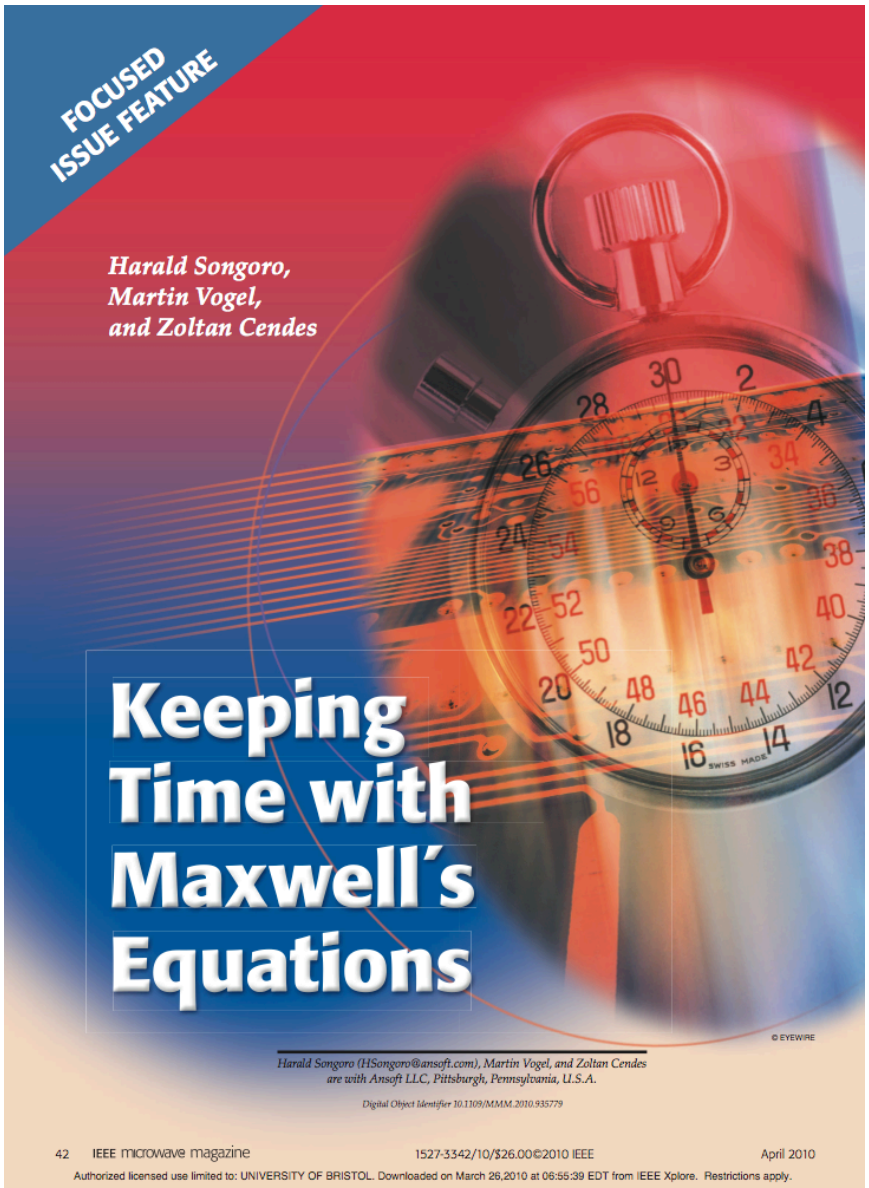

Introducing a commercial FETD solver breaks new ground in EM field simulation. Based on the DGTD method, it allows unstructured geometry-conforming meshes to be used for the first time in transient EM field simulation.

DGTD is a competitive alternative to traditional FDTD based methods to solving Maxwell's equations in the time domain. The applications presented here include the electromagnetic pulse susceptibility of the differential lines in a laptop computer, the radar signature of a landmine under undulating ground, the TDR of a bent flex circuit, and the return loss of a connector. All of these examples involve complicated, curved geometries where the flexibility of the unstructured meshes used in DGTD provides powerful advantages over simulation by conventional brick-shaped FDTD and FIT meshes.

IEEE Microwave Magazine - April 2010

Outline

Maxwell equations, $\mathbf{x} \in \Omega,\ t > 0$

$$\begin{cases} \varepsilon \partial_t \mathbf{E} - \nabla \times \mathbf{H} = 0 \\ \\ \mu \partial_t \mathbf{H} + \nabla \times \mathbf{E} = 0 \end{cases}$$

$$\mathbf{E} = \mathbf{E}(\mathbf{x}, t) \quad \text{and} \quad \mathbf{H} = \mathbf{H}(\mathbf{x}, t)$$

Boundary conditions: $\partial\Omega = \Gamma_a \cup \Gamma_m$

$$\begin{cases} \mathbf{n} \times \mathbf{E} = 0 \text{ on } \Gamma_m \\ \mathbf{n} \times \mathbf{E} - \sqrt{\dfrac{\mu}{\varepsilon}} \mathbf{n} \times (\mathbf{H} \times \mathbf{n}) = \mathbf{n} \times \mathbf{E}_{\text{inc}} - \sqrt{\dfrac{\mu}{\varepsilon}} \mathbf{n} \times (\mathbf{H}_{\text{inc}} \times \mathbf{n}) \text{ on } \Gamma_a \end{cases}$$

Initial conditions

$$\mathbf{E}_0 = \mathbf{E}(\mathbf{x}, 0) \quad \text{and} \quad \mathbf{H}_0 = \mathbf{H}(\mathbf{x}, 0)$$

Outline

- FDTD: Finite Difference Time-Domain method
- Seminal work of K.S. Yee
  (IEEE Trans. Antennas Propag., Vol. AP-14, 1966)
- Structured (cartesian) meshes
- Second order accurate (space and time) on uniform meshes
- Advantages
  - Easy computer implementation
  - Computationally efficient (very low algorithmic complexity)
  - Mesh generation is straightforward
  - Modelization of complex sources (antennas, thin wires, etc.) is well established
- Drawbacks
  - Accuracy on non-uniform discretizations
  - Memory requirements for high resolution models
  - Approximate discretization of boundaries (stair case representation)

Yee's scheme

- Staggered grid
- Non-dissipative scheme (centered in space and time)
- Second-order accurate in space and time (for a uniform grid)

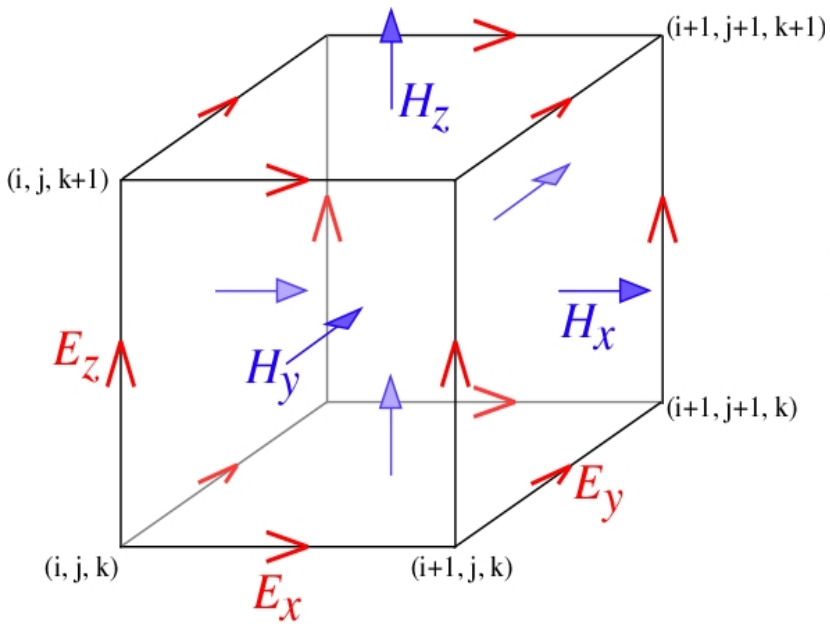

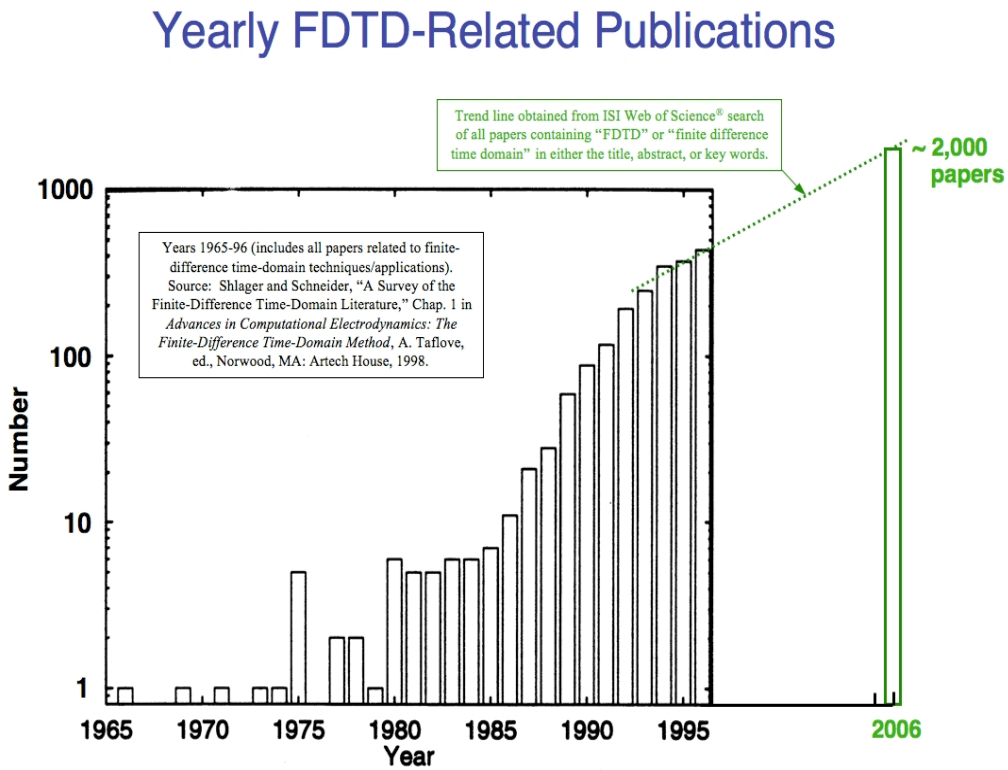

- FETD: Finite Element Time-Domain method
- Often based on J.-C. Nédélec edge elements (Numer. Math, Vol. 35, 1980 and Vol. 50, 1986)
  - Unstructured meshes
  - Advantages
    - Accurate representation of complex shapes
    - Well suited to high order interpolation methods
  - Drawbacks
    - Computer implementation is less trivial
    - Unstructured mesh generation is hardly automated
    - Global mass matrix
  - Mass lumped FETD methods
    - S. Pernet, X. Ferrieres and G. Cohen
      IEEE Trans. Antennas Propag., Vol. 53, No. 9, 2005
    - Hexahedral meshes, high order Lagrange polynomials
    - Leap-frog time integration scheme

- FIT : Finite Integration Technique
  - FIT was proposed in 1977 by Thomas Weiland and has been enhanced continually over the years
    (Electronics and Communications AEUE, Vol. 31, No. 3, 1977 and
    Numerical Modelling: Electronic Networks, Devices and Fields, Vol. 9, 1996)
  - The FIT is a spatial discretization scheme fo time- and frequency-domain problems
  - The basic idea is to solve the Maxwell equations in integral form on a set of staggered grids
  - It preserves basic topological properties of the continuous equations such as conservation of charge and energy
  - It covers the full range of electromagnetics (from static up to high frequency) and optic applications
  - It is implemented in the CST software suite

- FVTD: Finite Volume Time-Domain method
  - Imported from the computational fluid dynamics (CFD) community
    - V. Shankar, W. Hall and A. Mohammadian
      Electromag. Vol. 10, 1990
    - J.-P. Cioni, L. Fezoui and H. Steve
      IMPACT Comput. Sci. Eng., Vol. 5, No. 3, 1993
    - P. Bonnet, X. Ferrieres *et al.*
      J. Electromag. Waves and Appl., Vol. 11, 1997
    - S. Piperno and M. Remaki and L. Fezoui
      SIAM J. Num. Anal., Vol. 39, No. 6, 2002.
  - Unstructured meshes
  - Uknowns are cell averages of the field components
  - Flux evaluation at cell interfaces
    - Upwind scheme $\rightarrow$ numerical dissipation
    - Centered scheme $\rightarrow$ numerical dispersion (on non-uniform meshes)
  - Extension to higher order accuracy: MUSCL technique

- Initially introduced to solve neutron transport problems
  (W. Reed and T. Hill, 1973)
- Somewhere between a finite element and a finite volume method, gathering many good features of both
- Extensively developed by the CFD community
- Application to wave propagation problems naturally followed
- Reference text book
  J.S. Hesthaven and T. Warburton
  Nodal discontinuous Galerkin methods: algorithms, analysis, and applications
  Springer, 2008

- F. Bourdel, P.A. Mazet and P. Helluy
  Proc. 10th Inter. Conf. on Comp. Meth. in Appl. Sc. and Eng., 1992.
  - Triangular meshes, first-order upwind DG method (i.e FV method)
  - Time-domain and time-harmonic Maxwell equations
- M. Remaki and L. Fezoui, INRIA RR-3501, 1998.
  - Time-domain Maxwell equations
  - Triangular meshes, P1 interpolation, Runke-Kutta time integration (RKDG)
- J.S. Hesthaven and T. Warburton (J. Comput. Phys., Vol. 181, 2002)
  - Tetrahedral meshes, high order Lagrange polynomials, upwind flux
  - Runge-Kutta time integration
- B. Cockburn, F. Li and C.-W. Shu (J. Comput. Phys., Vol. 194, 2004)
  - Locally divergence-free discontinuous Galerkin formulation
- G. Cohen, X. Ferrieres and S. Pernet (J. Comput. Phys., Vol. 217, 2006)
  - Hexahedral meshes, high order Lagrange polynomials, penalized formulation
  - Leap-frog time integration scheme
- And a steadily increasing number of other works since 2005

ElectroScience Laboratory, The Ohio State University, USA

- Jin-Fa Lee *et al.*
- Interior penalty discontinuous Galerkin formulation
- Triangular (2D)/tetrahedral meshes, conformal PMLs
- Leap-frog time integration scheme, local time-stepping strategy
  - S. Dosopoulos and J.F. Lee. IEEE Trans. Ant. Propag., Vol. 58, 2010
  - S. Dosopoulos and J.F. Lee. J. Comput. Phys., Vol. 229, 2010

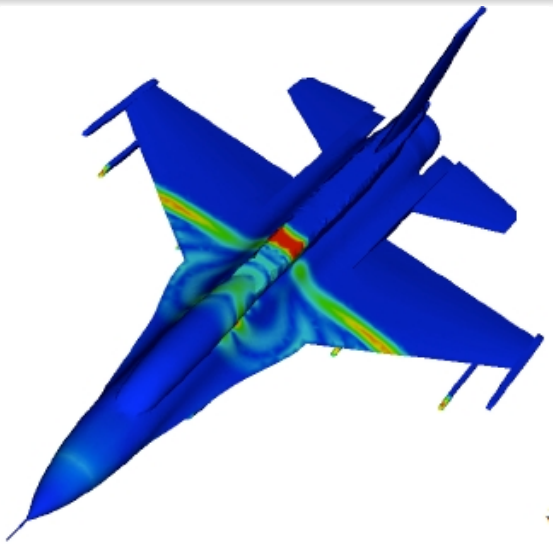

By courtesy of J.F. Lee

Computational Electromagnetics Group TU Darmstadt, Germany

- S. Schnepp, T. Weiland *et al.*
- Non-dissipative (centered flux) discontinuous Galerkin formulation
- Orthogonal quadrangular (2D)/hexahedral (3D) meshes
- Adpative mesh refinement
- Leap-frog time integration scheme
  - S. Schnepp and T. Weiland. Radio Science, Vol. 46, 2011

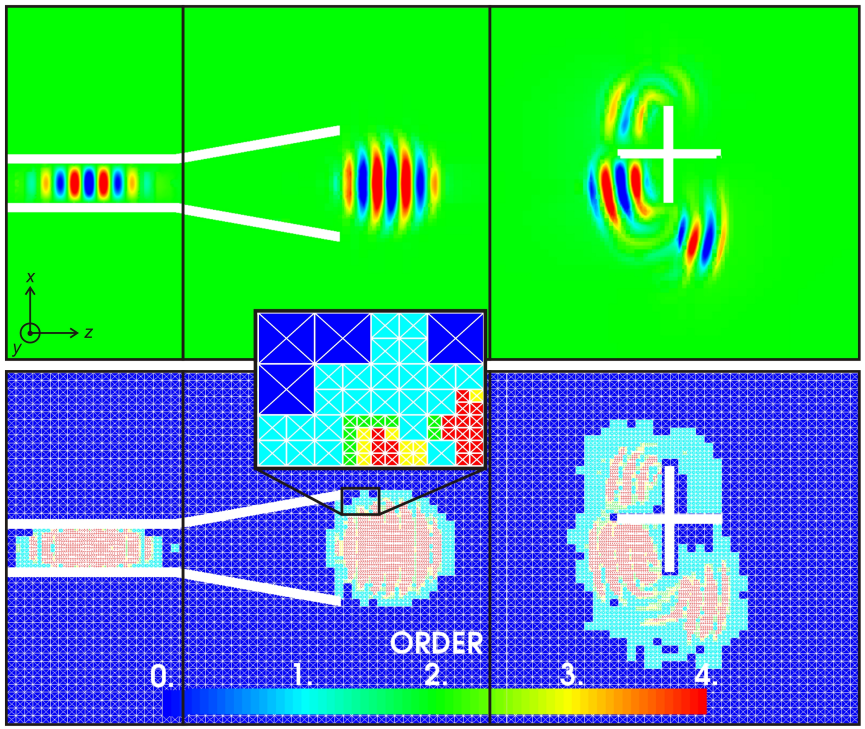

By courtesy of S. Schnepp

Discontinuous Galerkin Time Domain method

Photonics group, Institute for theoretical physics, University of Karlsruhe, Germany

- K. Busch, M. König and J. Niegemann
- Developement of discontinuous Galerkin methods for the efficient numerical treatment of nanophotonic systems

- Diffusive (upwind flux) discontinuous Galerkin formulation
- Triangular (2D)/tetrahedral meshes
- Runge-Kutta time integration
- Anisotropic materials
- Stretched-coordinate PMLs

- K. Busch, M. König and J. Niegemann
  Discontinuous Galerkin methods in nanophotonics
  Laser and Photonics Reviews, Vol. 5, No. 6, 2011
- M. König, K. Busch and J. Niegemann
  The discontinuous Galerkin time-domain method for Maxwell's equations with anisotropic materials
  Photonics and Nanostructures - Fundamentals and Applications, Vol. 8, 2010

Outline

DGTD-$\mathbb{P}_{p_i}$ method for the Maxwell equations

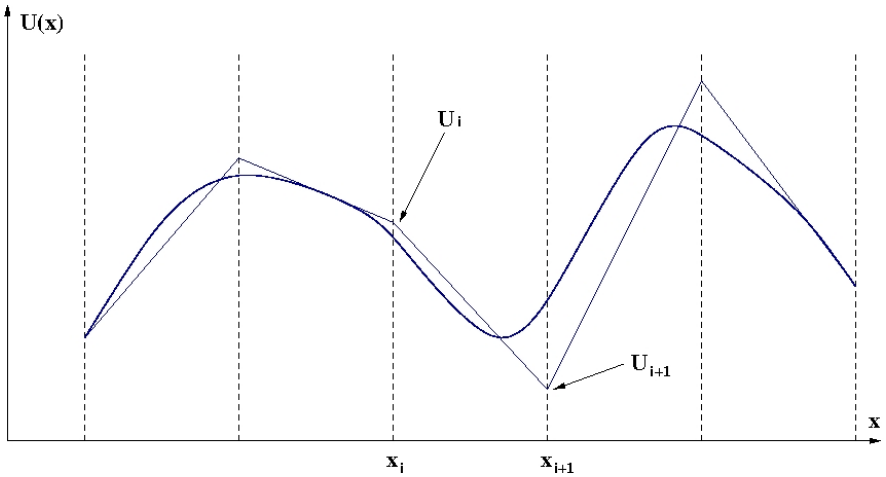

Continuous P1 interpolation

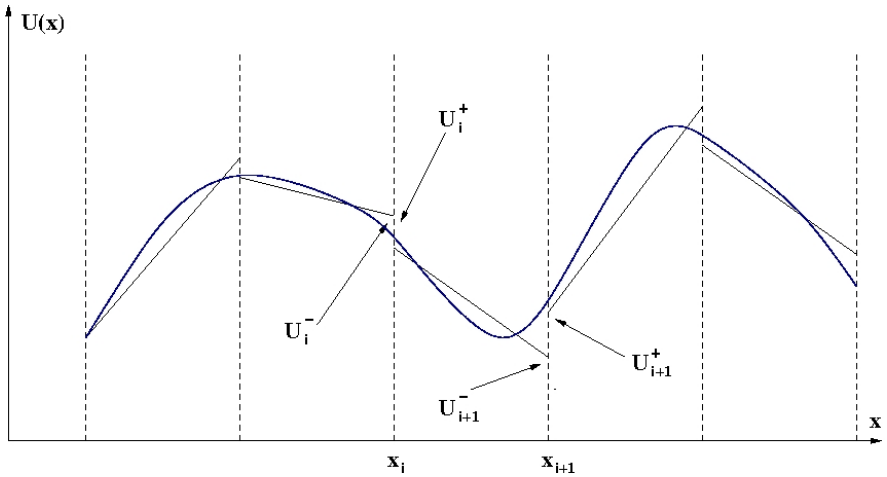

Discontinuous P1 interpolation

Motivations

- Naturally adapted to heterogeneous media and discontinuous solutions
- Can easily deal with unstructured, possibly non-conforming meshes (*h*-adaptivity)
- High order with compact stencils and non-conforming approximations (*p*-adaptivity)
- Usually rely on polynomial interpolation but can also accomodate alternative functions
- Yield block diagonal mass matrices when coupled to explicit time integration schemes
- Amenable to efficient parallelization
- But leads to larger problems compared to continuous finite element methods

- Disretization of Ω: $\overline{\Omega}_h \equiv \mathcal{T}_h = \bigcup_{\tau_i \in \mathcal{T}_h} \overline{\tau}_i$
  - $\mathcal{F}_0$: set of purely internal faces
  - $\mathcal{F}_m$ and $\mathcal{F}_a$: sets of faces on the boundaries Γ_m and Γ_a
- Approximation space: $V_h = \{\mathbf{V}_h \in L^2(\Omega)^3 \mid \forall i, \mathbf{V}_{h|\tau_i} \equiv \mathbf{V}_i \in \mathbb{P}_{p_i}[\tau_i]^3\}$
- Variational formulation: $\forall \vec{\varphi} \in \mathcal{P}_i = \text{Span}(\vec{\varphi}_{ij}\ ,\ 1 \leq j \leq d_i)$

$$\begin{cases} \displaystyle\iiint_{\tau_i} \vec{\varphi} \cdot \varepsilon_i \partial_t \mathbf{E} d\omega &= -\displaystyle\iint_{\partial\tau_i} \vec{\varphi} \cdot (\mathbf{H} \times \vec{n}) ds + \iiint_{\tau_i} \nabla \times \vec{\varphi} \cdot \mathbf{H} d\omega \\ \displaystyle\iiint_{\tau_i} \vec{\varphi} \cdot \mu_i \partial_t \mathbf{H} d\omega &= \displaystyle\iint_{\partial\tau_i} \vec{\varphi} \cdot (\mathbf{E} \times \vec{n}) ds - \iiint_{\tau_i} \nabla \times \vec{\varphi} \cdot \mathbf{E} d\omega \end{cases}$$

- Approximate fields: $\forall i$, $\mathbf{E}_{h|\tau_i} \equiv \mathbf{E}_i$ and $\mathbf{H}_{h|\tau_i} \equiv \mathbf{H}_i$
- Integral over $\partial\tau_i$: $\mathbf{E}_{|a_{ik}} = \dfrac{\mathbf{E}_i + \mathbf{E}_k}{2}$ and $\mathbf{H}_{|a_{ik}} = \dfrac{\mathbf{H}_i + \mathbf{H}_k}{2}$
- Assume $\Gamma_a = \emptyset$ (to simplify the presentation)
  and on Γ_m: $\mathbf{E}_{k|a_{ik}} = -\mathbf{E}_{i|a_{ik}}$ and $\mathbf{H}_{k|a_{ik}} = \mathbf{H}_{i|a_{ik}}$

$$
\begin{cases}
\displaystyle\iiint_{\tau_i} \vec{\varphi} \cdot \varepsilon_i \partial_t \mathbf{E}_i \, d\omega &= \dfrac{1}{2} \displaystyle\iiint_{\tau_i} (\nabla \times \vec{\varphi} \cdot \mathbf{H}_i + \nabla \times \mathbf{H}_i \cdot \vec{\varphi}) d\omega \\
&- \dfrac{1}{2} \displaystyle\sum_{k \in \mathcal{V}_i} \iint_{a_{ik}} \vec{\varphi} \cdot (\mathbf{H}_k \times \vec{n}_{ik}) ds \\
\displaystyle\iiint_{\tau_i} \vec{\varphi} \cdot \mu_i \partial_t \mathbf{H}_i \, d\omega &= -\dfrac{1}{2} \displaystyle\iiint_{\tau_i} (\nabla \times \vec{\varphi} \cdot \mathbf{E}_i + \nabla \times \mathbf{E}_i \cdot \vec{\varphi}) d\omega \\
&+ \dfrac{1}{2} \displaystyle\sum_{k \in \mathcal{V}_i} \iint_{a_{ik}} \vec{\varphi} \cdot (\mathbf{E}_k \times \vec{n}_{ik}) ds
\end{cases}
$$

- Local projections

$$\mathbf{E}_i(\mathbf{x}) = \sum_{1 \le j \le d_i} E_{ij} \vec{\varphi}_{ij}(\mathbf{x}) \quad \text{and} \quad \mathbf{H}_i(\mathbf{x}) = \sum_{1 \le j \le d_i} H_{ij} \vec{\varphi}_{ij}(\mathbf{x})$$

- $\vec{\varphi}_{ij}$: Lagrange (nodal) polynomials
- Vector representation of local fields

$$\mathbb{E}_i = \{E_{ij}\}_{1 \le j \le d_i} \text{ and } \mathbb{H}_i = \{H_{ij}\}_{1 \le j \le d_i}$$

- For $1 \le j, l \le d_i$:
  - $(\mathbf{M}_i^{\varepsilon})_{jl} = \varepsilon_i \iiint_{\tau_i} {}^{\mathsf{T}}\vec{\varphi}_{ij} \vec{\varphi}_{jl} d\omega \quad \text{and} \quad (\mathbf{M}_i^{\mu})_{jl} = \mu_i \iiint_{\tau_i} {}^{\mathsf{T}}\vec{\varphi}_{ij} \vec{\varphi}_{jl} d\omega$
  - $(\mathbf{K}_i)_{jl} = \frac{1}{2} \iiint_{\tau_i} ({}^{\mathsf{T}}\vec{\varphi}_{ij} \nabla \times \vec{\varphi}_{il} + {}^{\mathsf{T}}\vec{\varphi}_{il} \nabla \times \vec{\varphi}_{ij}) d\omega$

- For $1 \le j \le d_i \quad \text{and} \quad 1 \le l \le d_k$
  - $(\mathbf{S}_{ik})_{jl} = \frac{1}{2} \iint_{a_{ik}} {}^{\mathsf{T}}\vec{\varphi}_{ij} (\vec{\varphi}_{kl} \times \vec{n}_{ij}) ds$

Local EDO systems

$$\forall \tau_i \quad : \quad \begin{cases} \mathbf{M}_i^{\varepsilon} \dfrac{d\mathbb{E}_i}{dt} & = & \mathbf{K}_i \mathbb{H}_i & - & \displaystyle\sum_{k \in \mathcal{V}_i} \mathbf{S}_{ik} \mathbb{H}_k \\ \mathbf{M}_i^{\mu} \dfrac{d\mathbb{H}_i}{dt} & = & -\mathbf{K}_i \mathbb{E}_i & + & \displaystyle\sum_{k \in \mathcal{V}_i} \mathbf{S}_{ik} \mathbb{E}_k \end{cases}$$

Global EDO system (with $d = \sum_i d_i$)

$$\mathbf{M}^{\varepsilon} \frac{d\mathbb{E}}{dt} = \mathbf{G}\mathbb{H} \quad \text{and} \quad \mathbf{M}^{\mu} \frac{d\mathbb{H}}{dt} = -{}^{\mathsf{T}}\mathbf{G}\mathbb{E}$$

- $\mathbf{G} = \mathbf{K} - \mathbf{A} - \mathbf{B}$
- $\mathbf{M}^{\varepsilon}$ are $\mathbf{M}^{\mu}$ block diagonal symmetric definite positive matrices
- $\mathbf{K}$ is a $d \times d$ block diagonal symmetric matrix
- $\mathbf{A}$ is a $d \times d$ block sparse symmetric matrix (internal faces)
- $\mathbf{B}$ is a $d \times d$ block sparse skew symmetric matrix (metallic faces)

Local EDO systems

$$\forall \tau_i \quad : \quad \begin{cases} \mathbf{M}_i^{\varepsilon} \dfrac{d\mathbb{E}_i}{dt} & = & \mathbf{K}_i \mathbb{H}_i & - & \displaystyle\sum_{k \in \mathcal{V}_i} \mathbf{S}_{ik} \mathbb{H}_k \\ \mathbf{M}_i^{\mu} \dfrac{d\mathbb{H}_i}{dt} & = & -\mathbf{K}_i \mathbb{E}_i & + & \displaystyle\sum_{k \in \mathcal{V}_i} \mathbf{S}_{ik} \mathbb{E}_k \end{cases}$$

Global EDO system (with $d = \sum_i d_i$)

$$\mathbf{M}^{\varepsilon} \frac{d\mathbb{E}}{dt} = \mathbf{G}\mathbb{H} \quad \text{and} \quad \mathbf{M}^{\mu} \frac{d\mathbb{H}}{dt} = -{}^{\mathsf{T}}\mathbf{G}\mathbb{E}$$

- $\mathbf{G} = \mathbf{K} - \mathbf{A} - \mathbf{B}$
- $\mathbf{M}^{\varepsilon}$ are $\mathbf{M}^{\mu}$ block diagonal symmetric definite positive matrices
- $\mathbf{K}$ is a $d \times d$ block diagonal symmetric matrix
- $\mathbf{A}$ is a $d \times d$ block sparse symmetric matrix (internal faces)
- $\mathbf{B}$ is a $d \times d$ block sparse skew symmetric matrix (metallic faces)

Formulation

- L. Fezoui, S. Lanteri, S. Lohrengel and S. Piperno
  ESAIM: M2AN, Vol. 39, No. 6, 2005

$$\begin{cases} \mathbf{M}^{\varepsilon}\left(\dfrac{\mathbb{E}^{n+1}-\mathbb{E}^{n}}{\Delta t}\right) & = & \mathbf{G}\mathbb{H}^{n+\frac{1}{2}} \\ \mathbf{M}^{\mu}\left(\dfrac{\mathbb{H}^{n+\frac{1}{2}}-\mathbb{H}^{n-\frac{1}{2}}}{\Delta t}\right) & = & -{}^{\mathrm{T}}\mathbf{G}\mathbb{E}^{n+1} \end{cases}$$

Stability analysis

- Discrete electromagnetic energy
$$\mathcal{E}^{n} = {}^{\mathrm{T}}\mathbb{E}^{n}\mathbf{M}^{\varepsilon}\mathbb{E}^{n} + {}^{\mathrm{T}}\mathbb{H}^{n+\frac{1}{2}}\mathbf{M}^{\mu}\mathbb{H}^{n-\frac{1}{2}}$$
- Condition for $\mathcal{E}^{n}$ being a positive definite form
$$\Delta t \leq \frac{2}{d_2}, \quad \text{with} \quad d_2 = \| \, (\mathbf{M}^{-\mu})^{\frac{1}{2}} \; {}^{\mathrm{T}}\mathbf{G} \; (\mathbf{M}^{-\varepsilon})^{\frac{1}{2}} \, \|$$
- Extension to higher orfer leap-frog schemes
  H. Fahs and S. Lanteri
  J. Comput. Appl. Math., Vol. 234, 2010

Outline

The choice of the temporal integration is a crucial step for the global efficiency of the overall method

We distinguish two major families

1. Explicit integration methods
   - Result in less computational effort per time step
   - Lead to step size restrictions caused by the smallest element
2. Implicit integration methods
   - Lead in general to unconditional stability $\Rightarrow$ time step can be chosen arbitrarily large
   - Require the solution of large linear system $\Rightarrow$ high computational effort

A possible alternative is locally implicit time integration methods

- The smallest grid elements are treated implicitly
- The coarsest grid elements are treated explicitly

$\Rightarrow$ If the ratio of # fine to # coarse elements is small, the most severe step size restrictions are overcome

The choice of the temporal integration is a crucial step for the global efficiency of the overall method

We distinguish two major families

1. Explicit integration methods
   - Result in less computational effort per time step
   - Lead to step size restrictions caused by the smallest element
2. Implicit integration methods
   - Lead in general to unconditional stability $\Rightarrow$ time step can be chosen arbitrarily large
   - Require the solution of large linear system $\Rightarrow$ high computational effort

A possible alternative is locally implicit time integration methods

- The smallest grid elements are treated implicitly
- The coarsest grid elements are treated explicitly

$\Rightarrow$ If the ratio of # fine to # coarse elements is small, the most severe step size restrictions are overcome

Maxwell equations with source terms

$$\begin{cases} \varepsilon \partial_t \mathbf{E} - \nabla \times \mathbf{H} = \sigma \mathbf{E} - \mathbf{J}_E \\ \\ \mu \partial_t \mathbf{H} + \nabla \times \mathbf{E} = 0 \end{cases}$$

- ε, μ and σ are coefficients representing electric permittivity, magnetic permeability and electric conductivity, respectively
- $\mathbf{J}_E$ is a given source current

Discretization in space by a DG methd

$$\begin{cases} \mathbf{M}^{\varepsilon} \dfrac{d\mathbb{E}}{dt} & = & \mathbf{S}\mathbb{H} - \mathbf{D}^{\sigma}\mathbb{E} + \mathbf{M}^{\varepsilon}\mathbb{F}^{E} \\ \mathbf{M}^{\mu} \dfrac{d\mathbb{H}}{dt} & = & -{}^{\mathsf{T}}\mathbf{S}\mathbb{E} + \mathbf{M}^{\mu}\mathbb{F}^{H} \end{cases}$$

- $\mathbf{M}^{\varepsilon}$ and $\mathbf{M}^{\mu}$ are the mass matrices containing the values of the electric permittivity and magnetic permeability coefficient
- $\mathbf{S}$ emanates from the discretization of the curl operator
- $\mathbf{D}^{\sigma}$ is associated with the dissipative conduction term
- $\mathbb{F}^{E}$ and $\mathbb{F}^{H}$ are associated with source terms ($\mathbb{F}^{E}$ represents the given source current, but $\mathbb{F}^{E}$ and $\mathbb{F}^{H}$ may also contain Dirichlet boundary data)

We can give an equivalent formulation of the semi-discrete Maxwell system without mass matrices

It is obtained by a transformation based on the Cholesky decompositions of $\mathbf{M}^{\varepsilon}$ and $\mathbf{M}^{\mu}$

M.A. Botchev and J.G. Verwer SIAM J. Sci. Comput., Vol. 31, 2009

Discretization in space by a DG methd (without mass matrices)

$$\begin{cases} \dfrac{d\mathbb{E}}{dt} &= \mathbf{S}\mathbb{H} - \mathbf{D}^{\sigma}\mathbb{E} + \mathbb{F}^{E} \\ \dfrac{d\mathbb{H}}{dt} &= -{}^{\mathsf{T}}\mathbf{S}\mathbb{E} + \mathbb{F}^{H} \end{cases}$$

with adapted definitions of $\mathbb{E}$, $\mathbb{H}$, $\mathbf{S}$, $\mathbf{D}^{\sigma}$, $\mathbb{F}^{E}$ and $\mathbb{F}^{H}$

A popular integration method is the second order leap-frog scheme (LF2) that we can write in the three-stage form, emanating from Verlet's method

$$\begin{cases} \dfrac{\mathbb{H}^{n+\frac{1}{2}} - \mathbb{H}^{n}}{\Delta t/2} & = & -{}^{\mathrm{T}}\mathbf{S}\mathbb{E}^{n} + \mathbb{F}^{H}(t^{n}) \\ \dfrac{\mathbb{E}^{n+1} - \mathbb{E}^{n}}{\Delta t} & = & \mathbf{S}\mathbb{H}^{n+\frac{1}{2}} - \mathbf{D}\left(\dfrac{\mathbb{E}^{n} + \mathbb{E}^{n+1}}{2}\right) + \dfrac{\mathbb{F}^{H}(t^{n}) + \mathbb{F}^{H}(t^{n+1})}{2} \\ \dfrac{\mathbb{H}^{n+1} - \mathbb{H}^{n+\frac{1}{2}}}{\Delta t/2} & = & -{}^{\mathrm{T}}\mathbf{S}\mathbb{E}^{n+1} + \mathbb{F}^{H}(t^{n+1}) \end{cases}$$

This method is second order accurate, explicit, and conditionally stable with a critical time step size proportional to $h_{\min}$ determined by the smallest grid element

An alternative is the second order, unconditionally stable Crank-Nicolson method (CN2) that we write in the three-stage form

$$\begin{cases} \dfrac{\mathbb{H}^{n+\frac{1}{2}} - \mathbb{H}^{n}}{\Delta t/2} & = & -{}^{\mathrm{T}}\mathbf{S}\mathbb{E}^{n} + \mathbb{F}^{H}(t^{n}) \\ \dfrac{\mathbb{E}^{n+1} - \mathbb{E}^{n}}{\Delta t} & = & \mathbf{S}\mathbb{H}^{n+1} - \mathbf{D}\left(\dfrac{\mathbb{E}^{n} + \mathbb{E}^{n+1}}{2}\right) + \dfrac{\mathbb{F}^{H}(t^{n}) + \mathbb{F}^{H}(t^{n+1})}{2} \\ \dfrac{\mathbb{H}^{n+1} - \mathbb{H}^{n+\frac{1}{2}}}{\Delta t/2} & = & -{}^{\mathrm{T}}\mathbf{S}\mathbb{E}^{n+1} + \mathbb{F}^{H}(t^{n+1}) \end{cases}$$

This method is second order accurate and unconditionally stable

The expense for the implicit computation is too large to consider CN2 as an attractive alternative to LF2, especially in 3D

Hybrid explicit/implicit DGTD-$\mathbb{P}_p$ method

- S. Piperno, ESAIM: M2AN, Vol. 40, No. 5, 2006
- Explict scheme: Verlet method (i.e. three-step leap-frog method with **E** and **H** computed at the same time stations)
- Implicit scheme: Crank-Nicolson scheme
- Partitioning of the mesh elements into two subsets
  - $\mathcal{S}_e$: coarsest elements, treated explicitly
  - $\mathcal{S}_i$: smallest elements, treated implicitly

$$\mathbb{E} = \begin{pmatrix} \mathbb{E}_e \\ \mathbb{E}_i \end{pmatrix} \quad , \quad \mathbb{H} = \begin{pmatrix} \mathbb{H}_e \\ \mathbb{H}_i \end{pmatrix}$$

$$\mathbf{S} = \begin{pmatrix} \mathbf{S}_e & \mathbf{A}_{ei} \\ \mathbf{A}_{ie} & \mathbf{S}_i \end{pmatrix} \quad , \quad \mathbf{D} = \begin{pmatrix} \mathbf{D}_e^\sigma & \mathbf{O} \\ \mathbf{O} & \mathbf{D}_i^\sigma \end{pmatrix}$$

$$\mathbb{F}^E = \begin{pmatrix} \mathbb{F}_e^E \\ \mathbb{F}_i^E \end{pmatrix} \quad , \quad \mathbb{F}^H = \begin{pmatrix} \mathbb{F}_e^H \\ \mathbb{F}_i^H \end{pmatrix}$$

Hybrid explicit/implicit DGTD-$\mathbb{P}_p$ method

Inserting the splitting into the semi-discrete system we obtain the partitioned system of ODEs

$$\begin{cases} \dfrac{d\mathbb{E}_e}{dt} &= \mathbf{S}_e\mathbb{H}_e - \mathbf{A}_{ei}\mathbb{H}_i - \mathbf{D}_e^{\sigma}\mathbb{E}_e + \mathbb{F}_e^E \\ \dfrac{d\mathbb{E}_i}{dt} &= \mathbf{S}_i\mathbb{H}_i - \mathbf{A}_{ie}\mathbb{H}_e - \mathbf{D}_i^{\sigma}\mathbb{E}_i + \mathbb{F}_i^E \\ \dfrac{d\mathbb{H}_e}{dt} &= -{}^{\mathsf{T}}\mathbf{S}_e\mathbb{E}_e + {}^{\mathsf{T}}\mathbf{A}_{ie}\mathbb{E}_i + \mathbb{F}_e^H \\ \dfrac{d\mathbb{H}_i}{dt} &= -{}^{\mathsf{T}}\mathbf{S}_i\mathbb{E}_i + {}^{\mathsf{T}}\mathbf{A}_{ei}\mathbb{E}_e + \mathbb{F}_i^H \end{cases}$$

Hybrid explicit/implicit DGTD-$\mathbb{P}_p$ method

$$
\begin{cases}
\dfrac{\mathbb{H}_e^{n+\frac{1}{2}} - \mathbb{H}_e^{n}}{\Delta t/2} &= -{}^{\mathrm{T}}\mathbf{S}_e \mathbb{E}_e^{n} + {}^{\mathrm{T}}\mathbf{A}_{ie} \mathbb{E}_i^{n} + \mathbb{F}_e^{H}(t^n) \\
\dfrac{\mathbb{E}_e^{n+\frac{1}{2}} - \mathbb{E}_e^{n}}{\Delta t/2} &= \mathbf{S}_e \mathbb{H}_e^{n+\frac{1}{2}} - \mathbf{A}_{ei} \mathbb{H}_i^{n} - \mathbf{D}_e^{\sigma} \mathbb{E}_e^{n} + \mathbb{F}_e^{E}(t^n)
\end{cases}
$$

$$
\begin{cases}
\dfrac{\mathbb{E}_i^{n+1} - \mathbb{E}_i^{n}}{\Delta t} &= \mathbf{S}_i \left(\dfrac{\mathbb{H}_i^{n+1} + \mathbb{H}_i^{n}}{2} \right) - \mathbf{A}_{ie} \mathbb{H}_e^{n+\frac{1}{2}} - \mathbf{D}_i^{\sigma} \left(\dfrac{\mathbb{E}_i^{n+1} + \mathbb{E}_i^{n}}{2} \right) \\
&\quad + \dfrac{\mathbb{F}_i^{E}(t^n) + \mathbb{F}_i^{E}(t^{n+1})}{2} \\
\dfrac{\mathbb{H}_i^{n} - \mathbb{H}_i^{n+1}}{\Delta t} &= -{}^{\mathrm{T}}\mathbf{S}_i \left(\dfrac{\mathbb{E}_i^{n} + \mathbb{E}_i^{n+1}}{2} \right) + {}^{\mathrm{T}}\mathbf{A}_{ei} \mathbb{E}_e^{n+\frac{1}{2}} + \dfrac{\mathbb{F}_i^{H}(t^n) + \mathbb{F}_i^{H}(t^{n+1})}{2}
\end{cases}
$$

$$
\begin{cases}
\dfrac{\mathbb{E}_e^{n+1} - \mathbb{E}_e^{n+\frac{1}{2}}}{\Delta t/2} &= \mathbf{S}_e \mathbb{H}_e^{n+\frac{1}{2}} - \mathbf{A}_{ei} \mathbb{H}_i^{n+1} - \mathbf{D}_e^{\sigma} \mathbb{E}_e^{n+1} + \mathbb{F}_e^{E}(t^{n+1}) \\
\dfrac{\mathbb{H}_e^{n+1} - \mathbb{H}_e^{n+\frac{1}{2}}}{\Delta t/2} &= -{}^{\mathrm{T}}\mathbf{S}_e \mathbb{E}_e^{n+1} + {}^{\mathrm{T}}\mathbf{A}_{ie} \mathbb{E}_i^{n+1} + \mathbb{F}_e^{H}(t^{n+1})
\end{cases}
$$

Hybrid explicit/implicit DGTD-$\mathbb{P}_p$ method

- V. Dolean, H. Fahs, L. Fezoui and S. Lanteri
  J. Comput. Phys., Vol. 229, No. 2, 2010
- Stability analysis

$$\mathcal{E}^n = \mathcal{E}_e^n + \mathcal{E}_i^n + \mathcal{E}_h^n \quad \text{with} \quad \begin{cases} \mathcal{E}_e^n &= {}^{\mathrm{T}}\mathbb{E}_e^n \mathbf{M}_e^{\varepsilon} \mathbb{E}_e^n + {}^{\mathrm{T}}\mathbb{H}_e^{n+\frac{1}{2}} \mathbf{M}_e^{\mu} \mathbb{H}_e^{n-\frac{1}{2}} \\ \mathcal{E}_i^n &= {}^{\mathrm{T}}\mathbb{E}_i^n \mathbf{M}_i^{\varepsilon} \mathbb{E}_i^n + {}^{\mathrm{T}}\mathbb{H}_i^n \mathbf{M}_i^{\mu} \mathbb{H}_i^n \\ \mathcal{E}_h^n &= -\dfrac{\Delta t^2}{4} {}^{\mathrm{T}}\mathbb{H}_i^n {}^{\mathrm{T}}\mathbf{A}_{ei} (\mathbf{M}_e^{\varepsilon})^{-1} \mathbf{A}_{ei} \mathbb{H}_i^n \end{cases}$$

- Condition for $\mathcal{E}^n$ being a positive definite form

$$\Delta t \leq \frac{2}{\alpha_e + \max(\beta_{ei}, \gamma_{ei})} \quad \text{with} \quad \begin{cases} \alpha_e &= \| \, (\mathbf{M}_e^{\varepsilon})^{-\frac{1}{2}} \mathbf{S}_e (\mathbf{M}_e^{\mu})^{-\frac{1}{2}} \, \| \\ \beta_{ei} &= \| \, (\mathbf{M}_e^{\varepsilon})^{-\frac{1}{2}} \mathbf{A}_{ei} (\mathbf{M}_i^{\mu})^{-\frac{1}{2}} \, \| \\ \gamma_{ei} &= \| \, (\mathbf{M}_e^{\mu})^{-\frac{1}{2}} \mathbf{A}_{ei} (\mathbf{M}_i^{\varepsilon})^{-\frac{1}{2}} \, \| \end{cases}$$

Component splitting based hybrid explicit/implicit method
Collaboration with Jan Verwer, CWI

J. Verwer, BIT Numer. Math., Vol. 51, 2010

It is also a blend of LF2 and CN2 applied to the semi-discrete Maxwell system

$$\begin{cases} \dfrac{\mathbb{H}^{n+\frac{1}{2}} - \mathbb{H}^{n}}{\Delta t/2} & = & -{}^{\mathrm{T}}\mathbf{S}\mathbb{E}^{n} + \mathbb{F}^{H}(t^{n}) \\ \dfrac{\mathbb{E}^{n+1} - \mathbb{E}^{n}}{\Delta t} & = & \mathbf{S}_0\mathbb{H}^{n+\frac{1}{2}} + \mathbf{S}_1\left(\dfrac{\mathbb{H}^{n} + \mathbb{H}^{n+1}}{2}\right) - \mathbf{D}\left(\dfrac{\mathbb{E}^{n} + \mathbb{E}^{n+1}}{2}\right) \\ & + & \dfrac{\mathbb{F}^{H}(t^{n}) + \mathbb{F}^{H}(t^{n+1})}{2} \\ \dfrac{\mathbb{H}^{n+1} - \mathbb{H}^{n+\frac{1}{2}}}{\Delta t/2} & = & -{}^{\mathrm{T}}\mathbf{S}\mathbb{E}^{n+1} + \mathbb{F}^{H}(t^{n+1}) \end{cases}$$

for a general splitting $\mathbf{S} = \mathbf{S}_0 + \mathbf{S}_1$

$\mathbf{S}_1$ is defined as $\mathbf{S}_1 = \mathbf{S}\mathbf{S}_H$ where $\mathbf{S}_H$ is a diagonal matrix of dimension the length of $\mathbb{H}$ with,

$$(\mathbf{S}_H)_{jj} = \begin{cases} 0, & \text{component of } \mathbb{H} \text{ to be treated explicitly,} \\ 1, & \text{component of } \mathbb{H} \text{ to be treated implicitly.} \end{cases}$$

The second stage of the method leads to the solution of the linear system of equations,

$$\mathcal{M}\mathbb{E}^{n+1} = \mathbb{B}^{n+1}$$

where,

$$\begin{aligned} \mathcal{M} &= \mathcal{I} + \frac{\Delta t^2}{4}\mathbf{S}_1{}^{\mathsf{T}}\mathbf{S}_1 + \frac{\Delta t}{2}\mathbf{D}, \\ \mathbb{B}^{n+1} &= \mathbb{E}^n + \Delta t \mathbf{S}_0 \mathbb{H}^{n+\frac{1}{2}} + \frac{\Delta t}{2}\mathbf{S}_1\left(\mathbb{H}^n + \mathbb{H}^{n+\frac{1}{2}} + \frac{\Delta t}{2}\mathbb{F}^H(t^{n+1})\right) \\ &\quad - \frac{\Delta t}{2}\mathbf{D}\mathbb{E}^n + \frac{\Delta t}{2}\left(\mathbb{F}^E(t^n) + \mathbb{F}^E(t^{n+1})\right) \end{aligned}$$

$\Rightarrow$ The matrix $\mathcal{M}$ is significantly sparser than without splitting enabling to solve the linear system at a lower cost

Comparison of the two locally implicit methods

Convergence of J. Verwer's method

Let $\mathbb{F}^H(t)$, $\mathbb{F}^E(t) \in C^2[0,T]$ and suppose a Lax-Richtmyer stable space-time grid refinement $\Delta t \sim h$, $h \to 0$. On the interval $[0,T]$ the approximations $\mathbb{H}^n$ and $\mathbb{E}^n$ then converge with temporal order two to $\mathbb{H}_h(t)$ and $\mathbb{E}_h(t)$[a].

[a] $\mathbb{H}_h(t)$ and $\mathbb{E}_h(t)$ denote the true solutions of the underlying PDE problem restricted to the space grid.

Proof in J. Verwer, BIT Numer. Math., Vol. 51, 2010

Comparison of the two locally implicit methods

Convergence of S. Piperno's method

Let $\mathbb{F}^H(t)$, $\mathbb{F}^E(t) \in C^2[0,T]$ *and suppose a Lax-Richtmyer stable space-time grid refinement* $\Delta t \sim h$, $h \to 0$. *On* $[0,T]$ *the approximations* $\mathbb{H}_e^n$, $\mathbb{H}_i^n$, $\mathbb{E}_e^n$ *and* $\mathbb{E}_i^n$ *then converge to* $\mathbb{H}_{h,e}(t)$, $\mathbb{H}_{h,i}(t)$, $\mathbb{E}_{h,e}(t)$ *and* $\mathbb{E}_{h,i}(t)$

(*i*) *at least at first order*,

(*ii*) *at least at second order*, *if in addition*

$$^{\mathsf{T}}\mathbf{A}_{ei}\mathbf{S}_e\mathbb{H}_{h,e}(t) = \mathcal{O}\left(\frac{1}{\Delta t}\right) \text{ for } h \to 0.$$

Proof in L. Moya and J. Verwer, INRIA RR-7533, 2011

- 2D TMz Maxwell equations
- Propagation of an eigenmode in a unitary PEC cavity (no source terms)
- Boundary condition: $\mathbf{n} \times \mathbf{E} = 0$ on Γ_m
- DGTD-$\mathbb{P}_p$ method, non-uniform triangular mesh (# elements 2742)
- Comparison of fully explicit versus hybrid explicit/implicit (J. Verwer's scheme)

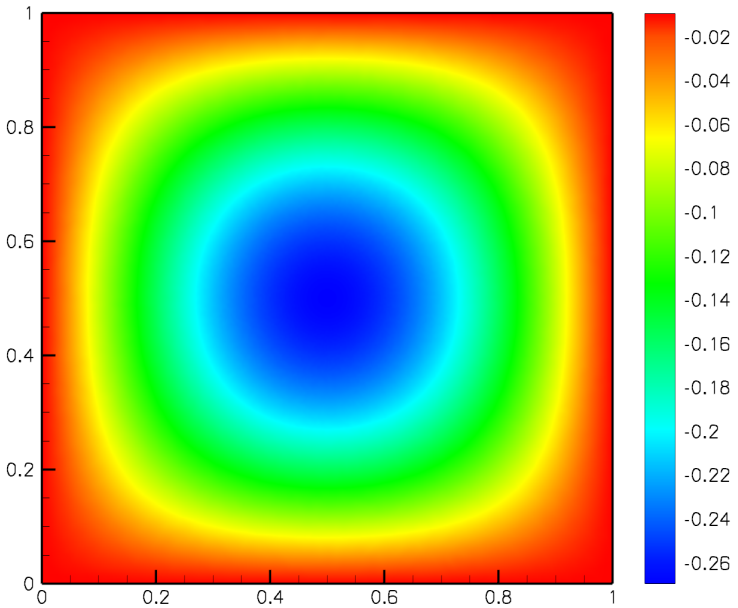

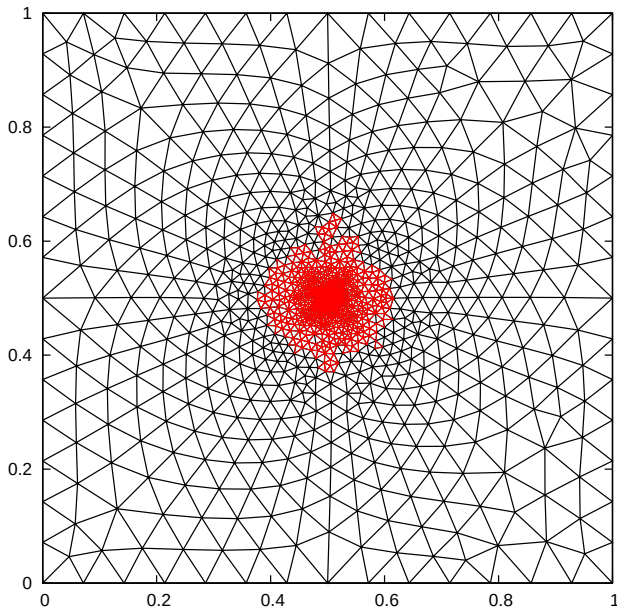

$\mathbb{P}_p$	# DOF	Δt_c (m)	# iter.	CPU (sec)	Max. L^2-error
$\mathbb{P}_4$	41130	0.3906e-4	25559	14337	0.1809e-6
	-	0.9869e-3	1014	836	0.1262e-5
$\mathbb{P}_3$	27420	0.5643e-4	17723	4670	0.7423e-5
	-	0.1425e-2	702	271	0.7868e-5
$\mathbb{P}_2$	16452	0.8681e-4	11520	1161	0.2886e-3
	-	0.2193e-2	456	71	0.2886e-3
$\mathbb{P}_1$	8226	0.1302e-3	7680	232	0.1306e-1
	-	0.3290e-2	304	15	0.1306e-1

$(\mathbb{P}_c$:$\mathbb{P}_s)$	# DOF	Δt_c (m)	# iter.	CPU (sec)	Max. L^2-error
$(\mathbb{P}_4$:$\mathbb{P}_3)$	33120	0.5643e-4	17723	6786	0.1837e-6
	-	0.9869e-3	1014	572	0.1261e-5
$(\mathbb{P}_4$:$\mathbb{P}_2)$	26712	0.8681e-4	11520	3331	0.1217e-5
	-	0.9869e-3	1014	433	0.1711e-5
$(\mathbb{P}_4$:$\mathbb{P}_1)$	21906	0.1302e-3	7680	1902	0.1257e-2
	-	0.9869e-3	1014	365	0.1257e-2
$(\mathbb{P}_3$:$\mathbb{P}_2)$	21012	0.8681e-4	11520	1911	0.7512e-5
	-	0.1425e-2	702	175	0.7952e-5
$(\mathbb{P}_3$:$\mathbb{P}_1)$	16206	0.1302e-3	7680	953	0.1280e-2
	-	0.1425e-2	702	130	0.1280e-2
$(\mathbb{P}_2$:$\mathbb{P}_1)$	11646	0.1302e-3	7680	458	0.1236e-2
	-	0.2193e-2	456	42	0.1236e-2

- Scattering of a plane wave by an airfoil profile
- Boundary conditions:

$$\begin{cases} \mathbf{n} \times \mathbf{E} = 0 \text{ on } \Gamma_m \\ \mathbf{n} \times \mathbf{E} - \sqrt{\frac{\mu}{\varepsilon}} \times (\mathbf{H} \times \mathbf{n}) = \mathbf{n} \times \mathbf{E}_{inc} - \sqrt{\frac{\mu}{\varepsilon}} \times (\mathbf{H}_{inc} \times \mathbf{n}) \text{ on } \Gamma_a \end{cases}$$

- DGTD-$\mathbb{P}_p$ method, non-uniform triangular mesh (# elements 5152)
- Comparison of fully explicit versus hybrid explicit/implicit (J. Verwer's scheme)

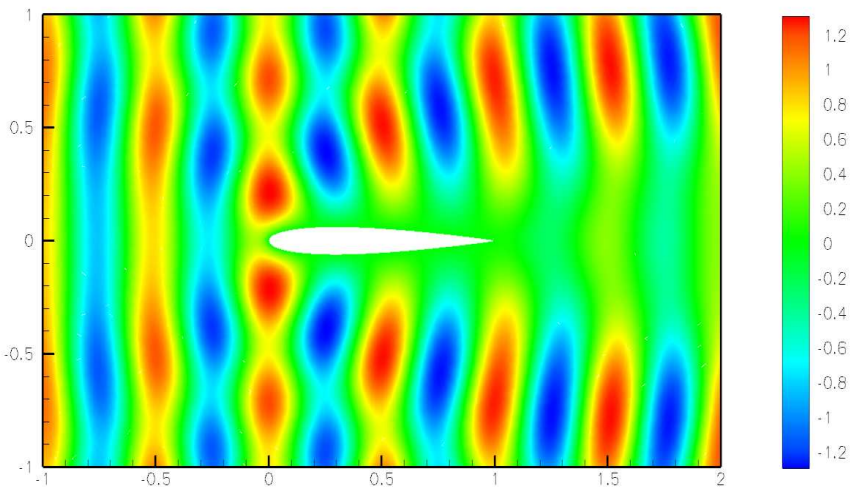

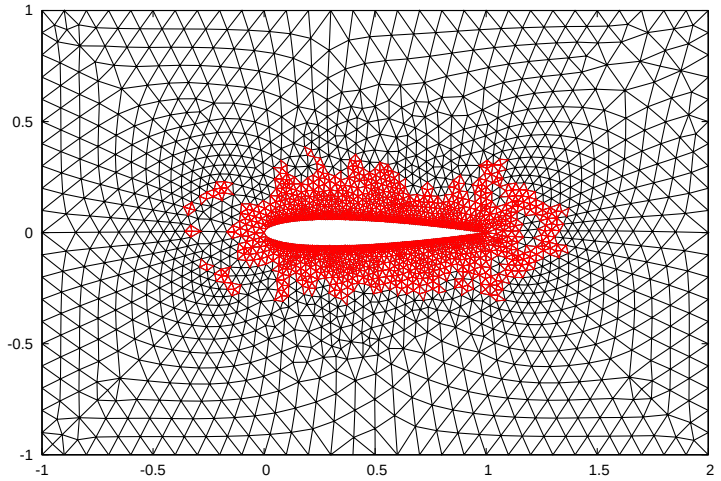

$\mathbb{P}_p$	# DOF	Δt_c (m)	# iter.	CPU (sec)
$\mathbb{P}_4$	77280	0.4061e-3	12320	25287
	-	0.2148e-2	2330	7110
$\mathbb{P}_3$	51520	0.5866e-3	8530	8000
	-	0.3103e-2	1620	2295
$\mathbb{P}_2$	30912	0.9025e-3	5560	1999
	-	0.4774e-2	1050	585
$\mathbb{P}_1$	15456	0.1353e-2	3700	392
	-	0.7161e-2	700	120

$(\mathbb{P}_c{:}\mathbb{P}_s)$	# DOF	Δt_c (m)	# iter.	CPU (sec)
$(\mathbb{P}_4{:}\mathbb{P}_3)$	62955	0.5866e-3	8530	12865
	-	0.2148e-2	2330	5175
$(\mathbb{P}_4{:}\mathbb{P}_2)$	51495	0.9025e-3	5550	6800
	-	0.2148e-2	2330	4135
$(\mathbb{P}_4{:}\mathbb{P}_1)$	42900	0.1353e-2	3700	4053
	-	0.2148e-2	2330	3654
$(\mathbb{P}_3{:}\mathbb{P}_2)$	40060	0.9025e-3	5550	3651
	-	0.3103e-2	1620	1582
$(\mathbb{P}_3{:}\mathbb{P}_1)$	31465	0.1353e-2	3700	1968
	-	0.3103e-2	1620	1259
$(\mathbb{P}_2{:}\mathbb{P}_1)$	22317	0.1353e-2	3700	875
	-	0.4774e-2	1050	376

Numerical results

- V. Dolean, H. Fahs, L. Fezoui and S. Lanteri
  J. Comput. Phys., Vol. 229, No. 2, 2010
- Scattering of plane wave (F=200 MHz, $\lambda = 1.5$ m) by an aircraft
- # vertices=360,495 and # elements=2,024,924
- Edges length: L_m=9.166 10^{-3} m ($\approx \lambda/163$ m) and L_M=6.831 10^{-1} m ($\approx \lambda/2.2$ m)
- Comparison of fully explicit versus hybrid explicit/implicit (S. Piperno's scheme)

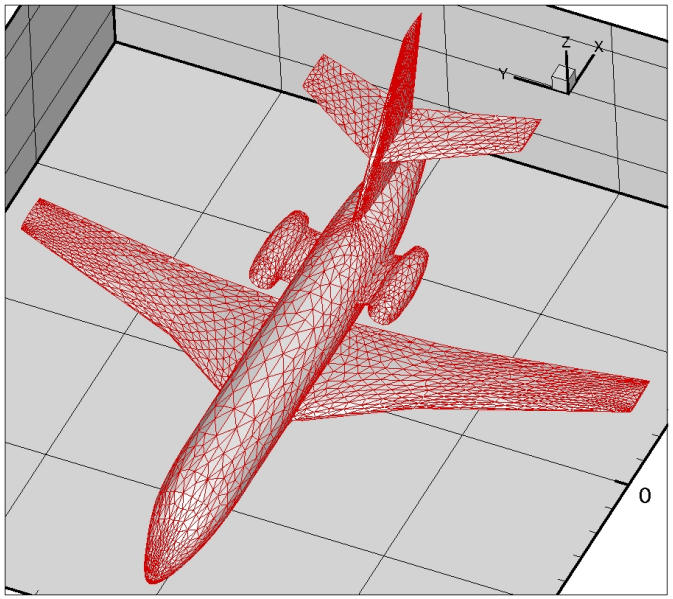

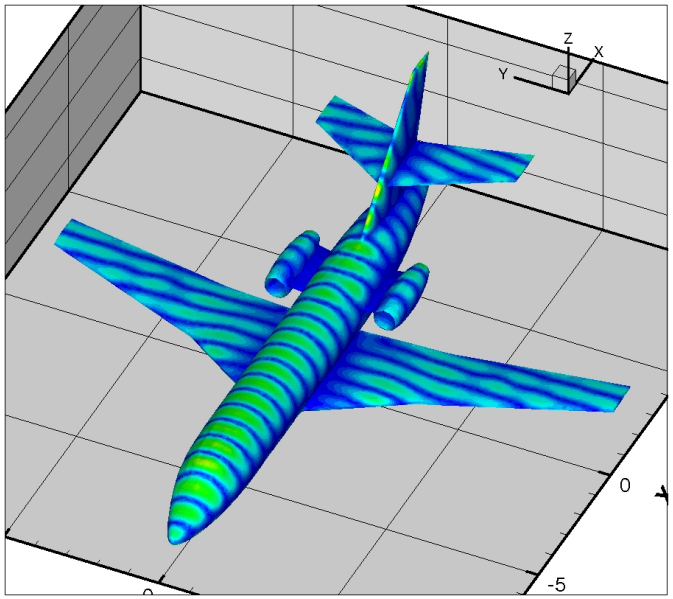

Hybrid explicit/implicit DGTD-$\mathbb{P}_p$ method

- Scattering of a plane wave (F=200 MHz, $\lambda = 1.5$ m) by an aircraft
- Geometric criterion: $\mathcal{C}(\tau_i) = 4 \min_{j \in \mathcal{V}_i} \sqrt{\frac{V_i V_j}{P_i P_j}}$
  - V_i , P_i: volume and perimeter of τ_i

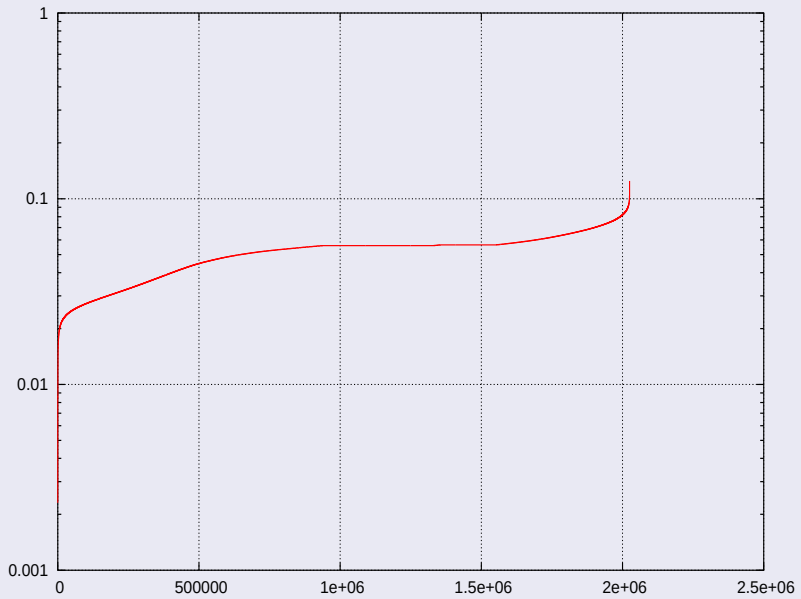

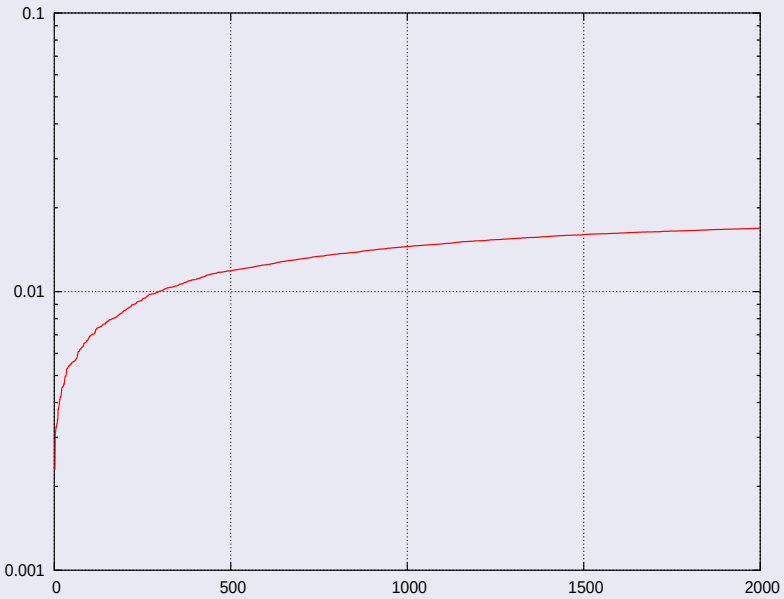

Distribution of the geometric criterion $\mathcal{C}$

Hybrid explicit/implicit DGTD-$\mathbb{P}_p$ method

- Scattering of a plane wave (F=200 MHz, $\lambda = 1.5$ m) by an aircraft

$\mathcal{C}$max	$\lvert\mathcal{S}_e\rvert$	$\lvert\mathcal{S}_i\rvert$
0.0125	2,024,320	604 (0.03 %)
0.0175	2,022,464	2,460 (0.12 %)
0.02	2,018,543	6,381 (0.31 %)

Definition of the subsets of explicit and implicit elements

$\mathcal{C}$max	RAM (LU)	Time (LU)	Time (total)
0.0125 m	12 MB	0.3 sec	6 h 39 mn
0.0175 m	48 MB	1.5 sec	4 h 44 mn
0.02 m	117 MB	4.2 sec	4 h 08 mn

Hybrid explicit-implicit DGTD-$\mathbb{P}_1$ method (Intel Xeon/2.33 GHz workstation)

Fully explicit DGTD-$\mathbb{P}_1$ method: 25 h 3 mn

Patch antenna problem

- DGTD method on locally-refined non-conforming cartesian grids
- In collaboration with France Telecom R&D, La Turbie research center
- N. Canouet, L. Fezoui and S. Piperno
  COMPEL, Vol. 24, No. 4, 2005

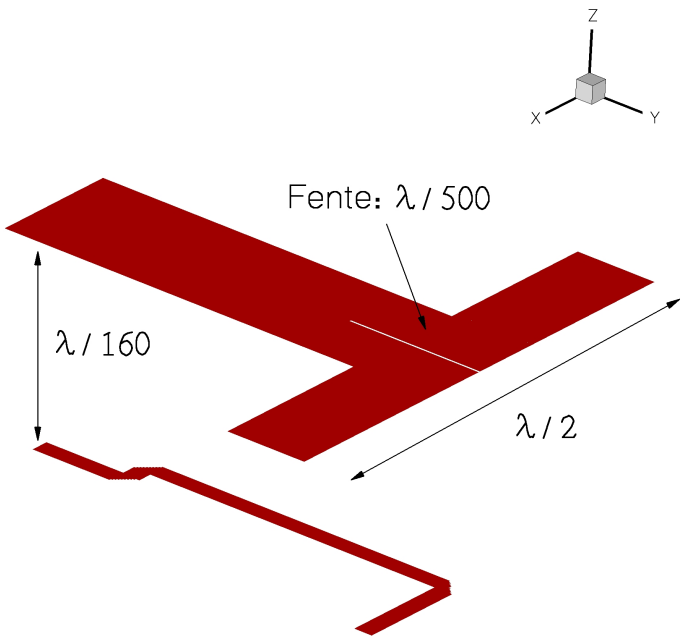

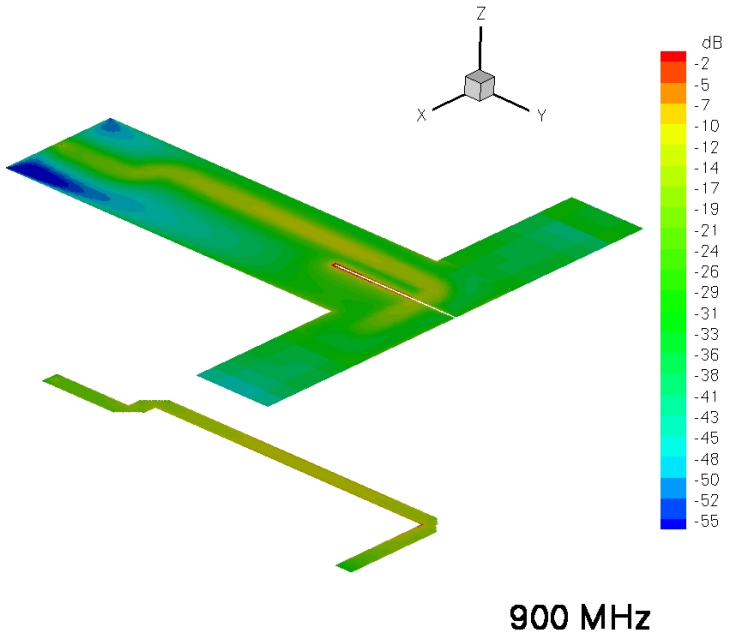

DGTD-$\mathbb{P}_p\mathbb{Q}_k$ method on hybrid structured-unstructured meshes

Motivations

- Improve the overall efficiency of DGTD-based simulations
- Simplify the mesh generation process of complex propagation scenes

Approach

- Domain partitioning
- Quadrangular (2D)/hexahedral (3D) orthogonal mesh for regions involving regularly shaped objects or vacuum zones
- Triangular (2D)/tetrahedral (3D) mesh for regions involving irregularly shaped objects
- Conforming versus non-conforming (i.e. with hanging nodes) discretization at the interface bewteen structured and unstructured mesh

Current achievements

- Formulation in 3D
- Stability and a priori convergence analysis
- Implementation in 2D (conforming and non-conforming meshes)

DGTD-$\mathbb{P}_p\mathbb{Q}_k$ method on hybrid structured-unstructured meshes

Motivations

- Improve the overall efficiency of DGTD-based simulations
- Simplify the mesh generation process of complex propagation scenes

Approach

- Domain partitioning
- Quadrangular (2D)/hexahedral (3D) orthogonal mesh for regions involving regularly shaped objects or vacuum zones
- Triangular (2D)/tetrahedral (3D) mesh for regions involving irregularly shaped objects
- Conforming versus non-conforming (i.e. with hanging nodes) discretization at the interface bewteen structured and unstructured mesh

Current achievements

- Formulation in 3D
- Stability and a priori convergence analysis
- Implementation in 2D (conforming and non-conforming meshes)

DGTD-$\mathbb{P}_p\mathbb{Q}_k$ method on hybrid structured-unstructured meshes

Motivations

- Improve the overall efficiency of DGTD-based simulations
- Simplify the mesh generation process of complex propagation scenes

Approach

- Domain partitioning
- Quadrangular (2D)/hexahedral (3D) orthogonal mesh for regions involving regularly shaped objects or vacuum zones
- Triangular (2D)/tetrahedral (3D) mesh for regions involving irregularly shaped objects
- Conforming versus non-conforming (i.e. with hanging nodes) discretization at the interface bewteen structured and unstructured mesh

Current achievements

- Formulation in 3D
- Stability and a priori convergence analysis
- Implementation in 2D (conforming and non-conforming meshes)

- Ω is discretized by $\mathscr{C}_h = \bigcup_{i=1}^{N} c_i = \mathscr{T}_h \bigcup \mathscr{Q}_h$, where c_i are tetrahedra ($\in \mathscr{T}_h$) or hexahedra ($\in \mathscr{Q}_h$) in 3D (triangles or quadrangles in 2D).
- $\mathbb{P}_p[c_i]$ the space of polynomial functions with degree at most p on $c_i \in \mathscr{T}_h$ ($\mathbb{P}_1$ function in 2D: $\xi_0 + \xi_1 x_1 + \xi_2 x_2$)
  $\mathbb{Q}_k[c_i]$ the space of polynomial functions with degree at most k with respect to each variable separately on $c_i \in \mathscr{Q}_h$ ($\mathbb{Q}_1$ function in 2D: $\gamma_0 + \gamma_1 x_1 + \gamma_2 x_2 + \gamma_3 x_1 x_2$)
- $\phi_i = (\varphi_{i1}, \varphi_{i2}, \ldots, \varphi_{id_i})$ local basis of $\mathbb{P}_p[c_i]$
  $\theta_i = (\vartheta_{i1}, \vartheta_{i2}, \ldots, \vartheta_{ib_i})$ local basis of $\mathbb{Q}_k[c_i]$
- Approximation space V_h^6 for $\mathbf{W}_h$

$$V_h = \left\{ \mathbf{V}_h \in L^2(\Omega) \;\middle|\; \begin{array}{l} \forall c_i \in \mathscr{T}_h,\ \mathbf{V}_h|_{c_i} \in \mathbb{P}_p[c_i] \\ \forall c_i \in \mathscr{Q}_h,\ \mathbf{V}_h|_{c_i} \in \mathbb{Q}_k[c_i] \end{array} \right\}$$

- Local degrees of freedom denoted by $\mathbf{W}_{il} \in \mathbb{R}^6$
- $\mathbf{W}_i$ defines the restriction of the approximate solution to the cell c_i $(\mathbf{W}_{h|_{c_i}})$
- $c_i \in \mathscr{T}_h \Longrightarrow \mathbf{W}_i \in \mathbb{P}_p[c_i]$: $\mathbf{W}_i(\mathbf{x}) = \sum_{l=1}^{d_i} \mathbf{W}_{il}\varphi_{il}(\mathbf{x}) \in \mathbb{R}^6$

  $c_i \in \mathscr{Q}_h \Longrightarrow \mathbf{W}_i \in \mathbb{Q}_k[c_i]$: $\mathbf{W}_i(\mathbf{x}) = \sum_{l=1}^{b_i} \mathbf{W}_{il}\vartheta_{il}(\mathbf{x}) \in \mathbb{R}^6$
- The local representation of $\mathbf{W}$ does not provide any form of continuity from one element to another. We use a centered numerical flux on $a_{ij} = c_i \cap c_j$

$$\mathbf{W}_{h|_{a_{ij}}} = \frac{\mathbf{W}_{i|_{a_{ij}}} + \mathbf{W}_{j|_{a_{ij}}}}{2}$$

Case A: c_i is a tetrahedron. a_{ij} face of c_i, is either on boundary, or common to another tetrahedron, or to a hexahedron (hybrid)
6d$_i$ semi-discretized equations system

$$\begin{cases} 2\mathcal{X}_{\varepsilon,i}\dfrac{d\overline{\mathbf{E}}_i}{dt} + \displaystyle\sum_{k=1}^{3}\mathcal{X}_i^{x_k}\overline{\mathbf{H}}_i + \sum_{a_{ij}\in\mathscr{T}_d^i}\mathcal{X}_{ij}\overline{\mathbf{H}}_j + \sum_{a_{ij}\in\mathscr{T}_m^i}\mathcal{X}_{im}\overline{\mathbf{H}}_i + \sum_{a_{ij}\in\mathscr{H}_d^i}\mathcal{A}_{ij}\tilde{\mathbf{H}}_j = 0 \\ 2\mathcal{X}_{\mu,i}\dfrac{d\overline{\mathbf{H}}_i}{dt} - \displaystyle\sum_{k=1}^{3}\mathcal{X}_i^{x_k}\overline{\mathbf{E}}_i - \sum_{a_{ij}\in\mathscr{T}_d^i}\mathcal{X}_{ij}\overline{\mathbf{E}}_j + \sum_{a_{ij}\in\mathscr{T}_m^i}\mathcal{X}_{im}\overline{\mathbf{E}}_i - \sum_{a_{ij}\in\mathscr{H}_d^i}\mathcal{A}_{ij}\tilde{\mathbf{E}}_j = 0 \end{cases}$$

with:

- $\overline{\mathbf{E}}_i = {}^t(\mathbf{E}_{i1}, \mathbf{E}_{i2}, \cdots, \mathbf{E}_{id_i})$ and $\overline{\mathbf{H}}_i = {}^t(\mathbf{H}_{i1}, \mathbf{H}_{i2}, \cdots, \mathbf{H}_{id_i}) \in \mathbb{R}^{3d_i}$
- $\tilde{\mathbf{E}}_j = {}^t(\mathbf{E}_{j1}, \mathbf{E}_{j2}, \cdots, \mathbf{E}_{jb_j})$ and $\tilde{\mathbf{H}}_j = {}^t(\mathbf{H}_{j1}, \mathbf{H}_{j2}, \cdots, \mathbf{H}_{jb_j}) \in \mathbb{R}^{3b_j}$
- $\mathcal{X}_{\varepsilon,i}$ and $\mathcal{X}_{\mu,i}$ are mass matrices, $\mathcal{X}_i^{x_k}$ gradient matrix, $\mathcal{X}_{ij}$ surface matrix
  $\Longrightarrow$ All have a $3d_i \times 3d_i$ size, except $\mathcal{A}_{ij}$, whose size is $3d_i \times 3b_j$

Case B: c_i is an hexahedron. a_{ij} face of c_i, is on boundary, or common to another hexahedron, or to a tetrahedron (hybrid)

6b$_i$ semi-discretized equations system

$$\begin{cases} 2\mathcal{W}_{\varepsilon,i}\dfrac{d\tilde{\mathbf{E}}_i}{dt} + \displaystyle\sum_{k=1}^{3}\mathcal{W}_i^{x_k}\tilde{\mathbf{H}}_i + \sum_{a_{ij}\in\mathcal{Q}_d^i}\mathcal{W}_{ij}\tilde{\mathbf{H}}_j + \sum_{a_{ij}\in\mathcal{Q}_m^i}\mathcal{W}_{im}\tilde{\mathbf{H}}_i + \sum_{a_{ij}\in\mathscr{H}_d^i}\mathcal{B}_{ij}\overline{\mathbf{H}}_j = 0 \\ 2\mathcal{W}_{\mu,i}\dfrac{d\tilde{\mathbf{H}}_i}{dt} - \displaystyle\sum_{k=1}^{3}\mathcal{W}_i^{x_k}\tilde{\mathbf{E}}_i - \sum_{a_{ij}\in\mathcal{Q}_d^i}\mathcal{W}_{ij}\tilde{\mathbf{E}}_j + \sum_{a_{ij}\in\mathcal{Q}_m^i}\mathcal{W}_{im}\tilde{\mathbf{E}}_i - \sum_{a_{ij}\in\mathscr{H}_d^i}\mathcal{B}_{ij}\overline{\mathbf{E}}_j = 0 \end{cases}$$

with:

- $\tilde{\mathbf{E}}_i = {}^t(\mathbf{E}_{i1}, \mathbf{E}_{i2}, \cdots, \mathbf{E}_{ib_i})$ and $\tilde{\mathbf{H}}_i = {}^t(\mathbf{H}_{i1}, \mathbf{H}_{i2}, \cdots, \mathbf{H}_{ib_i}) \in \mathbb{R}^{3b_i}$
- $\overline{\mathbf{E}}_j = {}^t(\mathbf{E}_{j1}, \mathbf{E}_{j2}, \cdots, \mathbf{E}_{jd_j})$ and $\overline{\mathbf{H}}_j = {}^t(\mathbf{H}_{j1}, \mathbf{H}_{j2}, \cdots, \mathbf{H}_{jd_j}) \in \mathbb{R}^{3d_j}$
- $\mathcal{W}_{\varepsilon,i}$ and $\mathcal{W}_{\mu,i}$ are mass matrices, $\mathcal{W}_i^{x_k}$ gradient matrix, $\mathcal{W}_{ij}$ surface matrix
  $\Longrightarrow$ All have a $3b_i \times 3b_i$ size, except $\mathcal{B}_{ij}$, whose size is $3b_i \times 3d_j$

Second order leap-frog scheme

- Case A:
$$\begin{cases} \overline{\mathbf{H}}_i^{n+\frac{1}{2}} = \overline{\mathbf{H}}_i^{n-\frac{1}{2}} + \dfrac{\Delta t}{2} \left[\mathcal{X}_{\mu,i}\right]^{-1} \mathbf{A}_{\mathbf{E},i}^{n} \\ \overline{\mathbf{E}}_i^{n+1} = \overline{\mathbf{E}}_i^{n} + \dfrac{\Delta t}{2} \left[\mathcal{X}_{\varepsilon,i}\right]^{-1} \mathbf{A}_{\mathbf{H},i}^{n+\frac{1}{2}} \end{cases}$$
- Case B:
$$\begin{cases} \tilde{\mathbf{H}}_i^{n+\frac{1}{2}} = \tilde{\mathbf{H}}_i^{n-\frac{1}{2}} + \dfrac{\Delta t}{2} \left[\mathcal{W}_{\mu,i}\right]^{-1} \mathbf{B}_{\mathbf{E},i}^{n} \\ \tilde{\mathbf{E}}_i^{n+1} = \tilde{\mathbf{E}}_i^{n} + \dfrac{\Delta t}{2} \left[\mathcal{W}_{\varepsilon,i}\right]^{-1} \mathbf{B}_{\mathbf{H},i}^{n+\frac{1}{2}} \end{cases}$$

Sability analysis

- We consider only metallic boundaries
- We define a discrete energy $\mathfrak{E}^n$ and we check that it is exactly conserved, i.e. $\Delta\mathfrak{E} = \mathfrak{E}^{n+1} - \mathfrak{E}^n = 0$
- We make hypotheses for fields in $(\mathbb{P}_p[c_i])^3$ and in $(\mathbb{Q}_k[c_i])^3$ to prove that $\mathfrak{E}^n$ is a positive definite quadratic form under a CFL condition
- For the DGTD-$\mathbb{P}_p$ method, the sufficient condition on Δt_τ is,

$$\forall i, \forall j \in \mathcal{V}_i : \; t_\tau \left[2\alpha_i^\tau + \beta_{ij}^\tau \max\left(\sqrt{\varepsilon_i/\varepsilon_j}, \sqrt{\mu_i/\mu_j} \right) \right] \; < \; \frac{4|c_i|\sqrt{\varepsilon_i \mu_i}}{p_i}$$

- A similar condition on Δt_q can be proved for DGTD-$\mathbb{Q}_k$ method (with α_i^q and β_{ij}^q)

Finally, noting Δt the global time step for the hybrid method, we have shown that a sufficient stability condition is defined by,

$$\Delta t = \min(\Delta t_\tau, \Delta t_q)$$

Under this condition and hypothesis, $\mathfrak{E}^n$ is a positive definite quadratic form

A priori convergence analysis

- Let $\mathbf{W}_h \in \mathcal{C}^1([0,t_f];V_h^6)$ and let $\mathbf{W} \in \mathcal{C}^0([0,t_f];(PH^{s+1}(\Omega))^6)$ for $s \leq 0$ with t_f the final time and,

$$PH^{s+1}(\Omega) = \{v \mid \forall j, v_{|c_j} \in H^{s+1}(c_j)\}$$

- Let $h_\tau = \max_{\tau_i \in \mathcal{T}_h}(h_{\tau_i})$, $h_q = \max_{q_i \in \mathcal{Q}_h}(h_{q_i})$ and,

$$\eta_h = \max\left\{h_\tau^{\min\{s,p\}}, h_q^{\min\{s,k\}}\right\}$$

- We found that the error of the semi-discretized problem is of order $\mathcal{O}(t_f\eta_h)$
- The fully discretized scheme may be seen as the discretization in time of a system of ODEs. Since the leap-frog scheme is second-order accurate, we found that the consistency error is of order $\mathcal{O}(\Delta t^2)$
- Finally, together with the stability result we thus get an error of order (if the exact solution is regular enough),

$$\mathcal{O}(\Delta t^2) + \mathcal{O}(t_f\eta_h)$$

- 2D TMz Maxwell equations
- Eigenmode in a unitary PEC square cavity

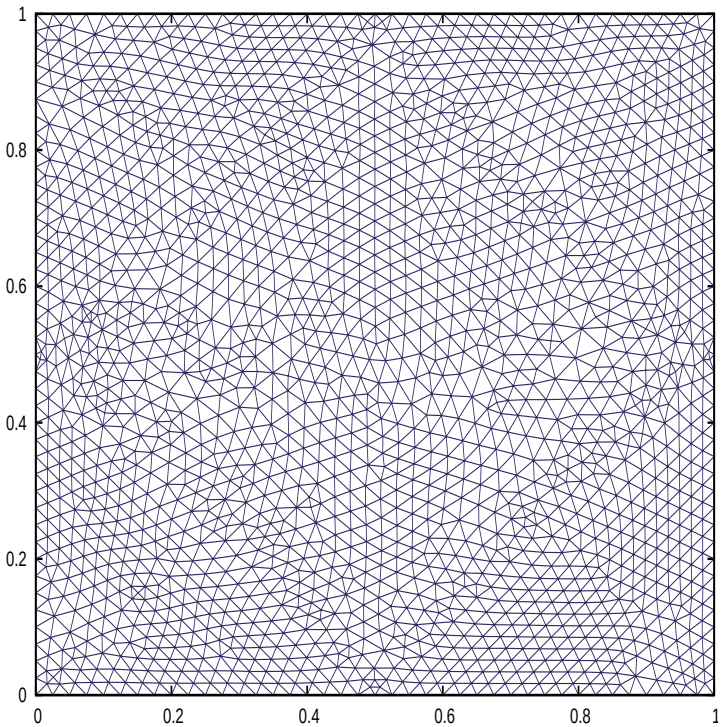

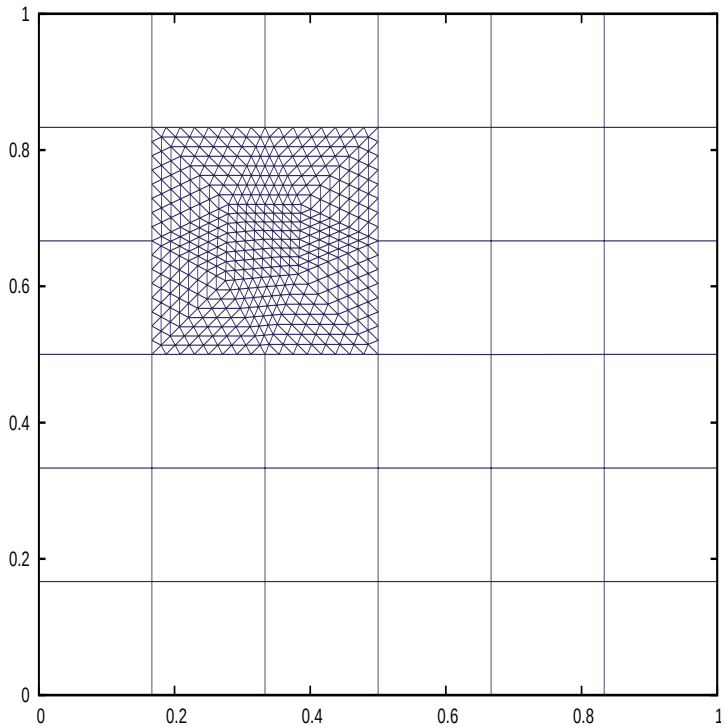

- 2D TMz Maxwell equations
- Eigenmode in a unitary PEC square cavity

Type of mesh	Interpolation order	CPU time	# DOF	Final L^2-error
Triangular	DGTD-$\mathbb{P}_1$	45 sec	11334	2.33×10^{-2}
	DGTD-$\mathbb{P}_2$	206 sec	22668	1.68×10^{-4}
	DGTD-$\mathbb{P}_3$	530 sec	37780	7.09×10^{-5}
	DGTD-$\mathbb{P}_4$	1511 s	56670	2.94×10^{-5}
Hybrid	DGTD-$\mathbb{P}_1\mathbb{Q}_4$	11 sec	3488	4.03×10^{-3}
	DGTD-$\mathbb{P}_2\mathbb{Q}_3$	38 sec	5888	3.39×10^{-4}
	DGTD-$\mathbb{P}_3\mathbb{Q}_4$	122 sec	9760	9.96×10^{-5}
	DGTD-$\mathbb{P}_4\mathbb{Q}_4$	318 sec	14240	5.07×10^{-5}

- 2D TMz Maxwell equations
- Eigenmode in a unitary PEC square cavity
- Numerical convergence study

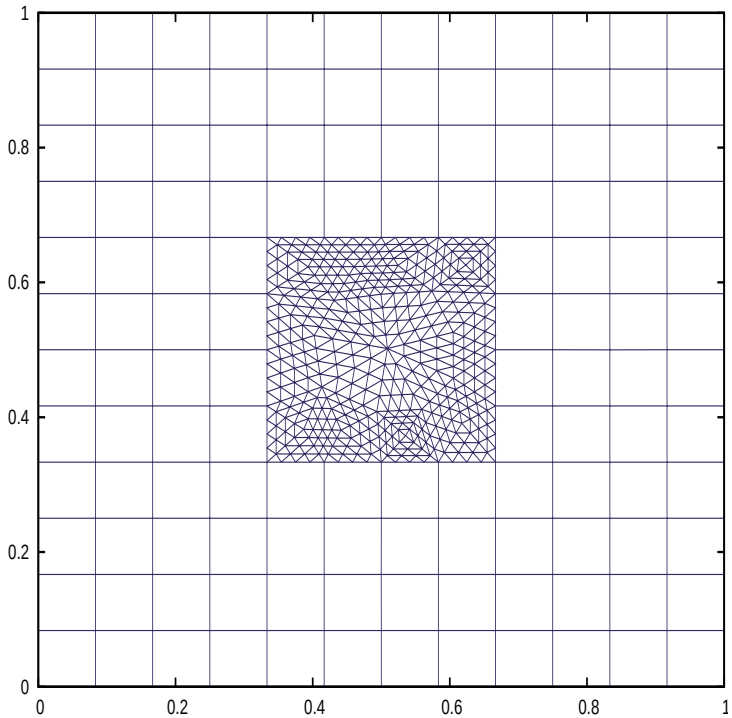

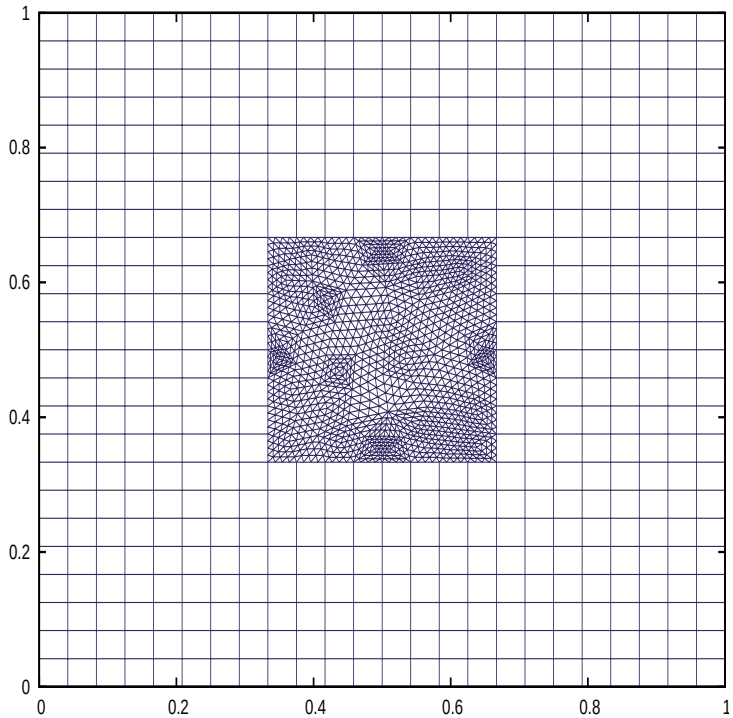

- 2D TMz Maxwell equations
- Eigenmode in a unitary PEC square cavity
- Numerical convergence study

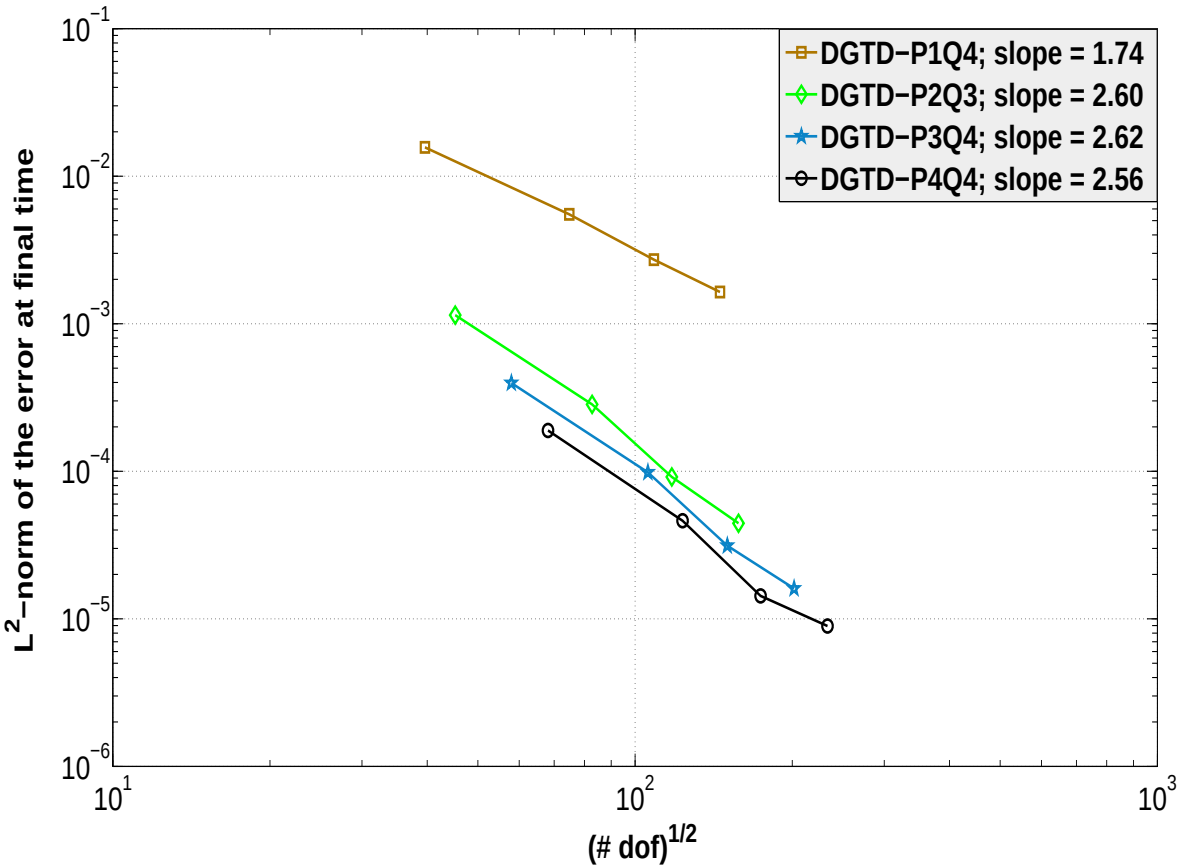

DGTD-$\mathbb{P}_p\mathbb{Q}_k$ method on hybrid structured-unstructured meshes

- Scattering of a plane wave (F=600 MHz) by a PEC cylinder
- Triangular mesh: # triangles=3276
- Hybrid quadrangular-triangular mesh: # quadrangles=192 and # triangles=2656

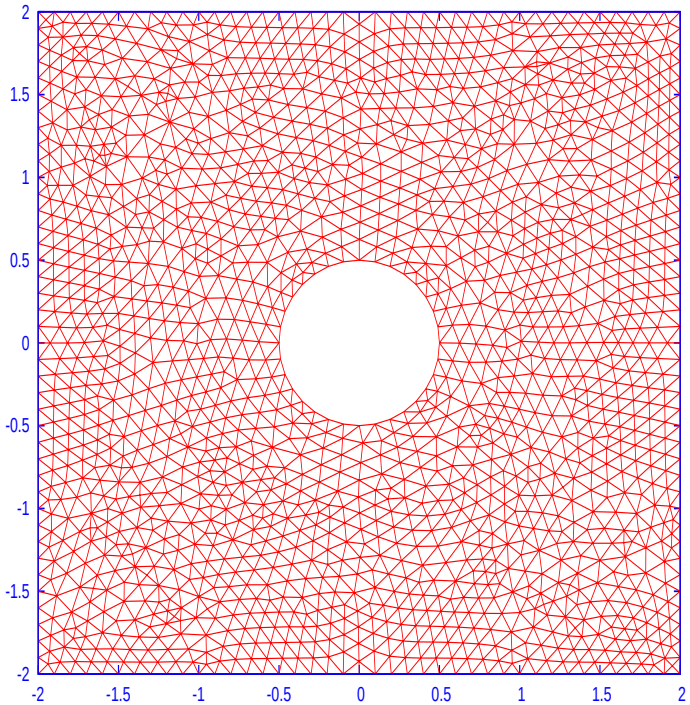

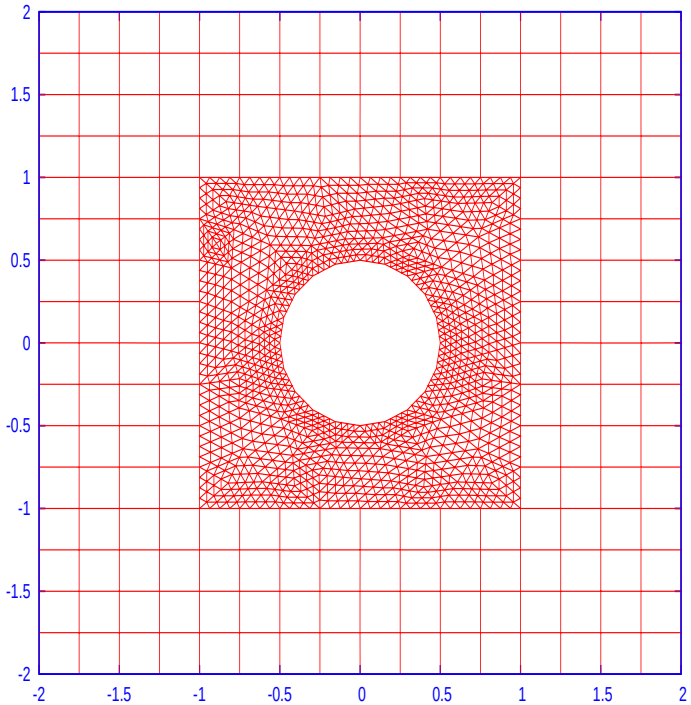

DGTD-$\mathbb{P}_p\mathbb{Q}_k$ method on hybrid structured-unstructured meshes

- Scattering of a plane wave (F=600 MHz) by a PEC cylinder
- DGTD-$\mathbb{P}_3$ method: 19.7 sec
- DGTD-$\mathbb{P}_2\mathbb{Q}_4$ method: 8.2 sec

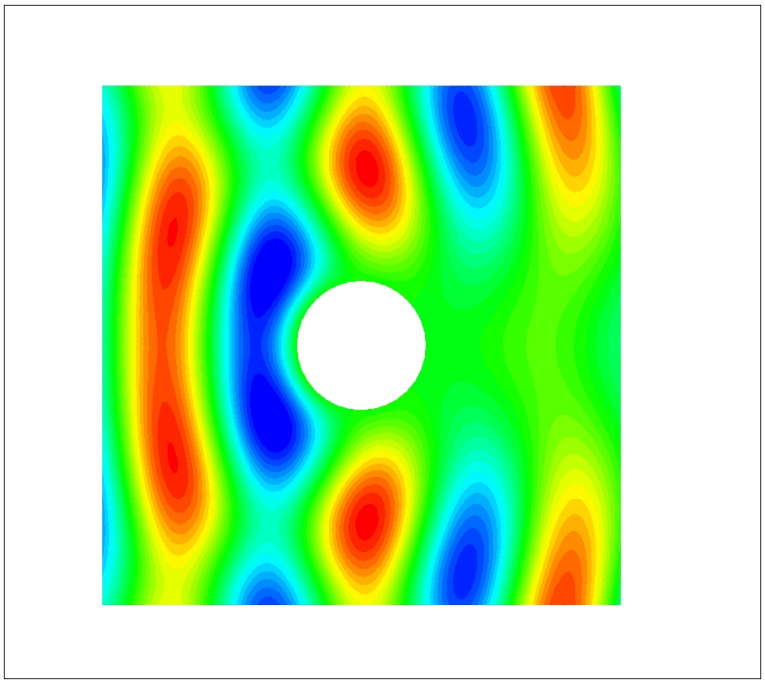

DGTD-$\mathbb{P}_3$ method

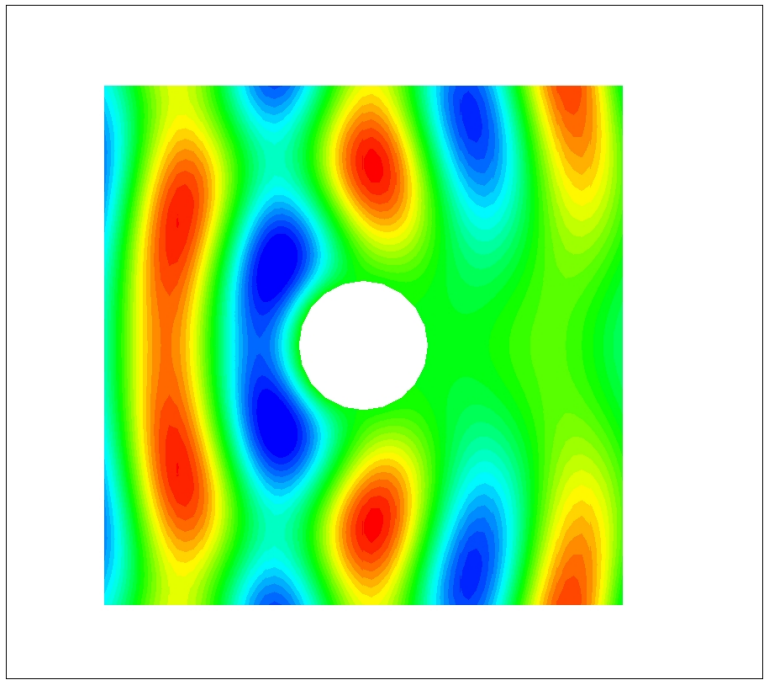

DGTD-$\mathbb{P}_2\mathbb{Q}_4$ method

Context

- One year old collaboration with Centre for Communications Research, Department of Electrical and Electric Engineering University of Bristol (Maciej Klemm)
- Biomedical application: microwave radar-based medical imaging
- Specific objectives
  1. Propagation of electromagnetic waves in biological tissues
  2. Numerical treatment of complex antenna arrays

Current status

- Development of a DGTD method for Debye type dispersive model
- ADE (Auxiliary Differential Equation) approach
- Direct extension of the method devised for non-dispersive media
- Stability and convergence analysis
- Preliminary numerical investigation on simple model problems

Context

- One year old collaboration with Centre for Communications Research, Department of Electrical and Electric Engineering University of Bristol (Maciej Klemm)
- Biomedical application: microwave radar-based medical imaging
- Specific objectives
  1. Propagation of electromagnetic waves in biological tissues
  2. Numerical treatment of complex antenna arrays

Current status

- Development of a DGTD method for Debye type dispersive model
- ADE (Auxiliary Differential Equation) approach
- Direct extension of the method devised for non-dispersive media
- Stability and convergence analysis
- Preliminary numerical investigation on simple model problems

Dynamic microwave neuro-functional brain imaging

- Brain activation leads to an increase in the metabolism of its neuronal cells, accompanied via neurovascular coupling by an increase in the cerebral blood flow (CBF), cerebral blood volume (CBV) and oxygen consumption
- fEIT[a] studies have shown conductivity changes of 2% to 4%
- Semenov *al.*[b] have shown that a microwave system is capable of detecting (in vivo) changes in blood flow as small as 1%

$\Rightarrow$ DMI radar should detect it!

[a] functional Electrical Impedance Tomography
[b] Phys. Med. Biol., Vol. 52, 2007).

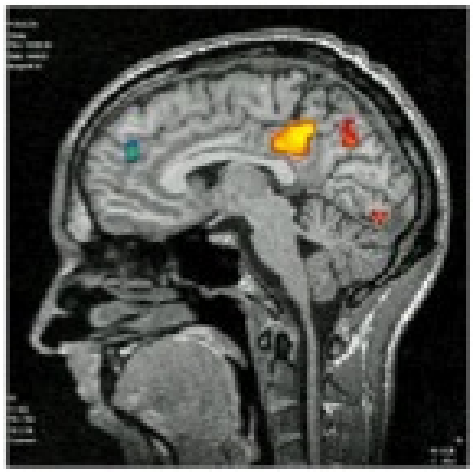

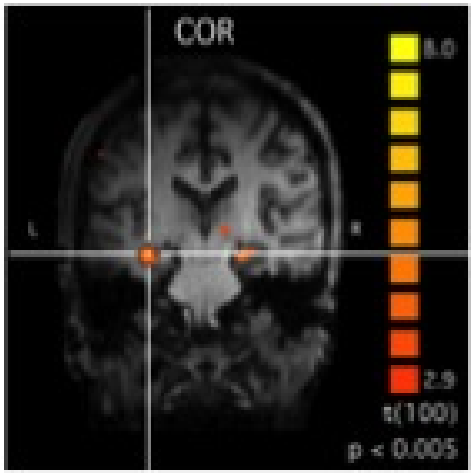

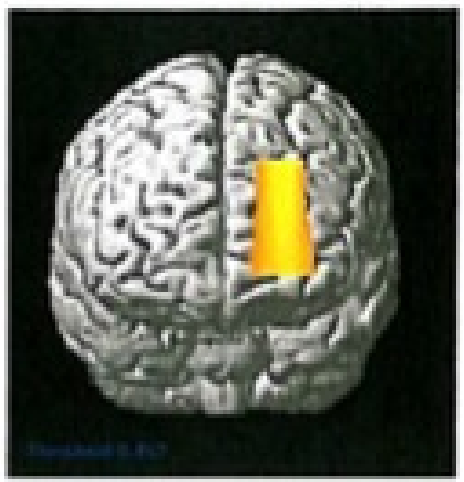

Some recent realizations or ongoing studies

Ongoing effort: realistic numerical models of head tissues
+ DGDT method for dispersive media

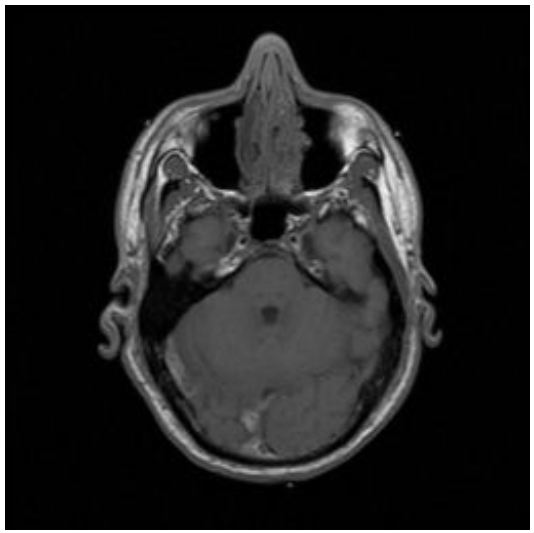

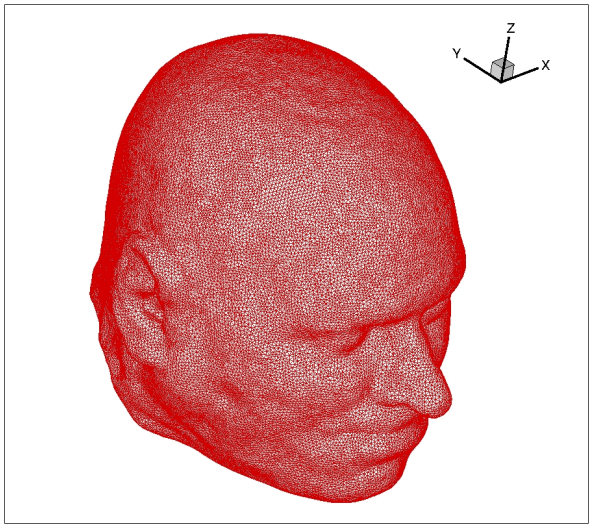

Geometric models

- Built from segmented medical images
- Extraction of surfacic (triangular) meshes of the tissue interfaces using specific tools
  - Marching cubes + adaptive isotropic surface remeshing
  - Delaunay refinement
- Generation of tetrahedral meshes using a Delaunay/Voronoi tool

Some recent realizations or ongoing studies

A biomedical application

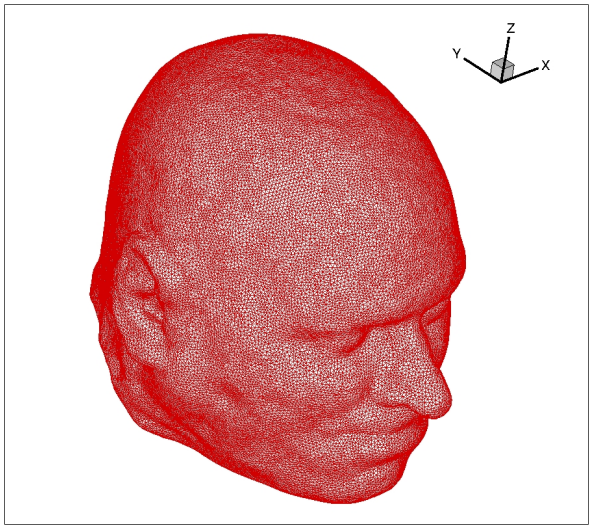

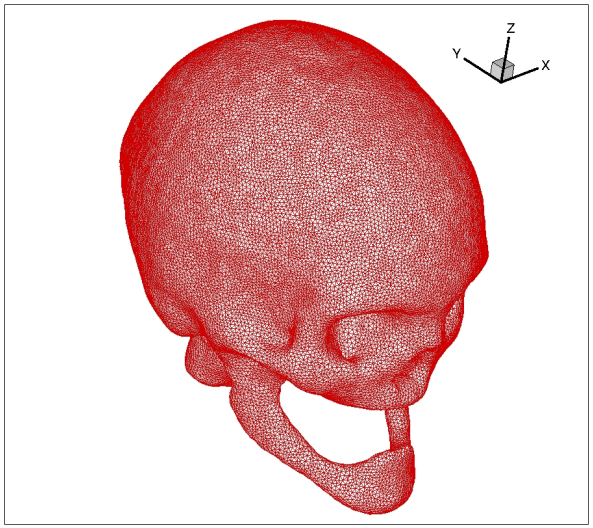

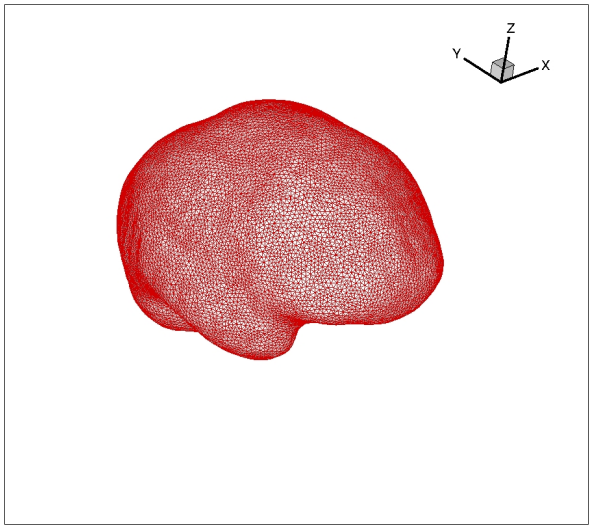

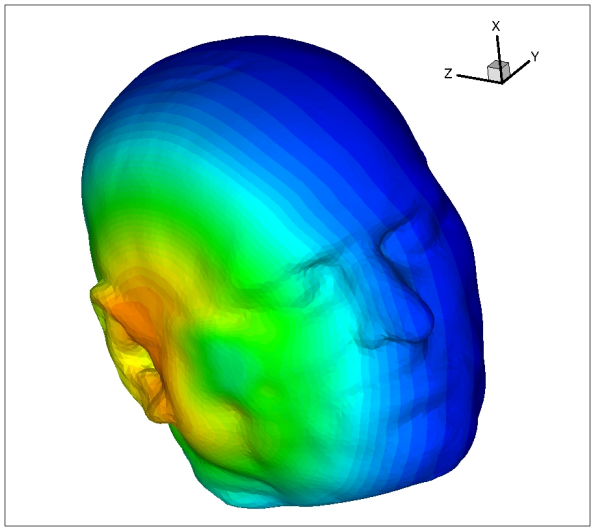

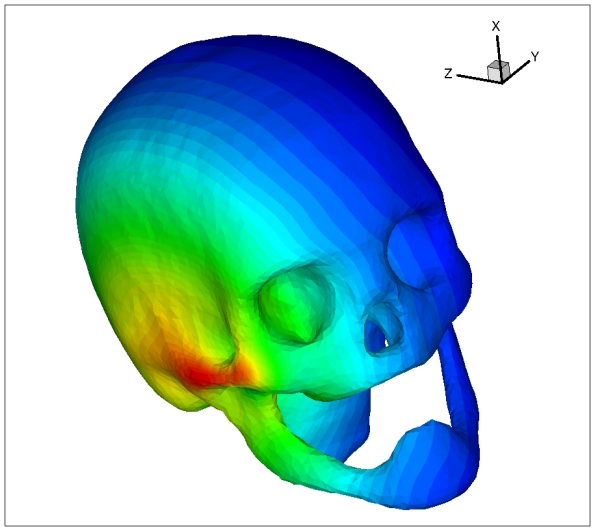

Governing equations for a Debye model

$$\begin{cases} \mu \dfrac{\partial \mathbf{H}}{\partial t} + \nabla \times \mathbf{E} = 0 \\ \varepsilon_0 \varepsilon_\infty \dfrac{\partial \mathbf{E}}{\partial t} - \nabla \times \mathbf{H} = -\dfrac{1}{\tau_r} \left[\varepsilon_0 \left(\varepsilon_s - \varepsilon_\infty \right) \mathbf{E} - \mathbf{P} \right] - \sigma \mathbf{E} \\ \dfrac{\partial \mathbf{P}}{\partial t} = \dfrac{1}{\tau_r} \left[\varepsilon_0 \left(\varepsilon_s - \varepsilon_\infty \right) \mathbf{E} - \mathbf{P} \right] \end{cases}$$

where:
ε_∞ is the relative electric permittivity of the medium at infinite frequency,
ε_s is the static, low frequency permittivity,
τ_r is the characteristic relaxation time of the medium.

DGTD method for dispersive media

- Centered flux discontinuous Galerkin scheme
- Leap-frog based explicit time-stepping
- C. Scheid and S. Lanteri, INRIA preprint RR-7634

$$\forall \tau_i \quad : \quad \begin{cases} \mathbf{M}_i^{\varepsilon} \dfrac{d\mathbb{E}_i}{dt} = \mathbf{K}_i \mathbb{H}_i - \displaystyle\sum_{k \in \mathcal{V}_i} \mathbf{S}_{ik} \mathbb{H}_k \\ \mathbf{M}_i^{\mu} \dfrac{d\mathbb{H}_i}{dt} = -\mathbf{K}_i \mathbb{E}_i + \displaystyle\sum_{k \in \mathcal{V}_i} \mathbf{S}_{ik} \mathbb{E}_k \end{cases}$$

GPU accelerated DGTD method

- DG method bulding blocks: matrix-vector products with dense (or almost dense) matrices
- Dense linear algebra particularly well suited to SIMD architecture of a GPU
- Local nature and mixed sparse-dense structure of a DG method calls for hybrid MIMD-SIMD computing

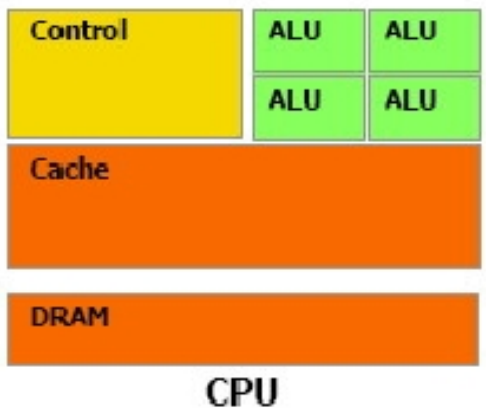

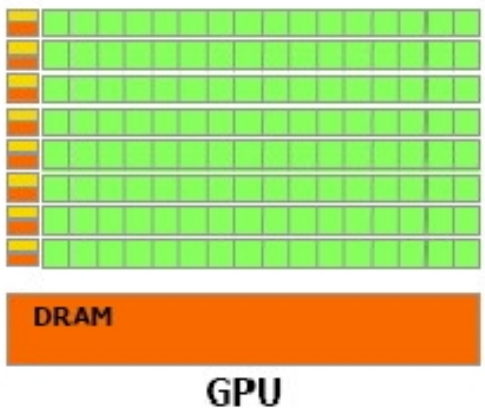

Implementation

Each DGTD time iteration can be decomposed into 3 steps applied at the element level

Development of CUDA-enabled kernels

1. Compute step: $\mathbb{X}_i^1 = \mathbf{K}_i \mathbb{H}_i^{n+\frac{1}{2}}$
2. Compute step: $\mathbb{X}_i^2 = \sum_{k \in \mathcal{V}_i} \mathbf{S}_{ik} \mathbb{H}_k^{n+\frac{1}{2}}$
3. Update step: $\mathbb{E}_i^{n+1} = \mathbb{E}_i^n + \Delta t (\mathbf{M}_i^\varepsilon)^{-1} (\mathbb{X}_i^1 - \mathbb{X}_i^2)$

Parallelization strategy for clusters of CPUs

Domain partitioning + message passing programming (MPI)

Model test problem and configurations

Hardware: cluster with 1024 Intel CPU nodes (2 quad-core Intel Xeon X5570 Nehalem processors - 2.93 GHz) and 48 Teslas S1070 GPU systems with four GT200 GPUs

Propagation of a standing wave in a perfectly conducting unitary cubic cavity

Regular uniform tetrahedral meshes respectively containing 3,072,000 elements for the DGTD-$\mathbb{P}_1$ and DGTD-$\mathbb{P}_2$ methods, 1,296,000 elements for the DGTD-$\mathbb{P}_3$ method and 750,000 elements for the DGTD-$\mathbb{P}_4$ method

Boxwise domain decompositions with optimal computational load balance

Computational performances

# GPU	DGTD-$\mathbb{P}_1$	DGTD-$\mathbb{P}_2$	DGTD-$\mathbb{P}_3$	DGTD-$\mathbb{P}_4$
1	63 GFlops	92 GFlops	106 GFlops	94 GFlops
128	8072 GFlops	11844 GFlops	13676 GFlops	12009 GFlops

Model test problem and configurations

Hardware: cluster with 1024 Intel CPU nodes (2 quad-core Intel Xeon X5570 Nehalem processors - 2.93 GHz) and 48 Teslas S1070 GPU systems with four GT200 GPUs

Propagation of a standing wave in a perfectly conducting unitary cubic cavity

Regular uniform tetrahedral meshes respectively containing 3,072,000 elements for the DGTD-$\mathbb{P}_1$ and DGTD-$\mathbb{P}_2$ methods, 1,296,000 elements for the DGTD-$\mathbb{P}_3$ method and 750,000 elements for the DGTD-$\mathbb{P}_4$ method

Boxwise domain decompositions with optimal computational load balance

Computational performances

# GPU	DGTD-$\mathbb{P}_1$	DGTD-$\mathbb{P}_2$	DGTD-$\mathbb{P}_3$	DGTD-$\mathbb{P}_4$
1	63 GFlops	92 GFlops	106 GFlops	94 GFlops
128	8072 GFlops	11844 GFlops	13676 GFlops	12009 GFlops

GPU-enabled high performance computing

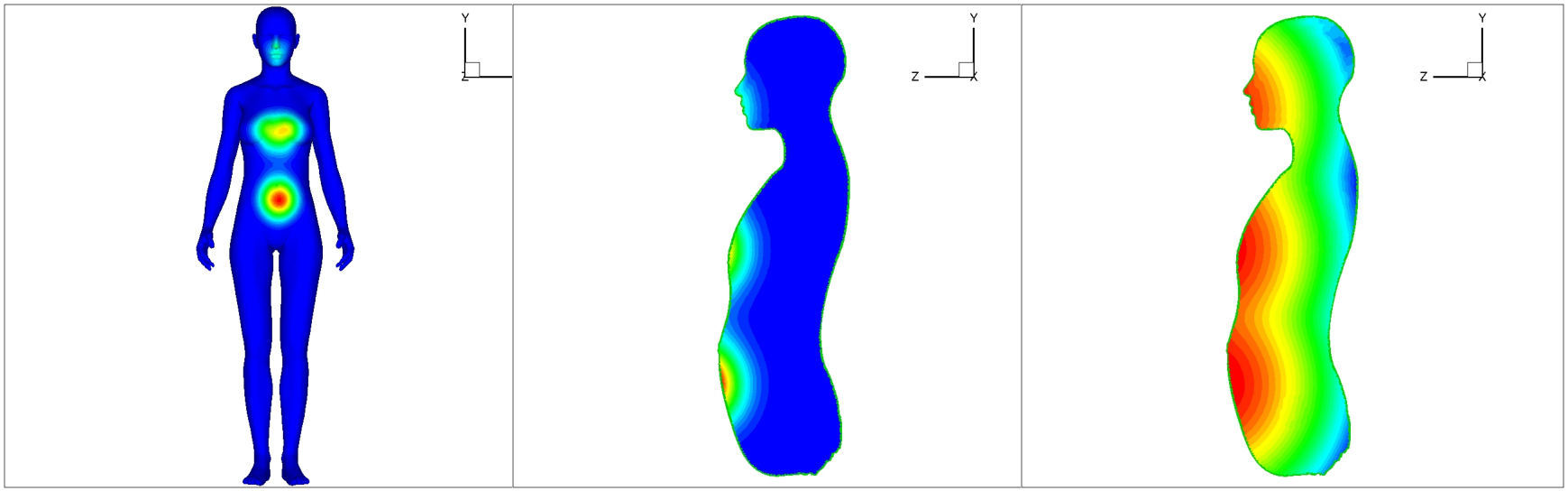

- Mesh: # elements = 5,536,852
- Total # DOF is 132,884,448 (DGTD-$\mathbb{P}_1$ method) and 332,211,120 (DGTD-$\mathbb{P}_2$ method)
- Time on 64 CPU cores for the DGTD-$\mathbb{P}_1$ method: 7 h 10 mn

# GPU	DGTD-$\mathbb{P}_1$			DGTD-$\mathbb{P}_2$		
	Time	GFlops	Speedup	Time	GFlops	Speedup
64	12 mn	2762	-	59 mn	4525	-
128	7 mn	4643	1.7	30 mn	8865	1.95

Outline

Closure: ongoing and future works

- Numerical treatment of grid-induced stiffness
  - Extension to 3D of hybrid explicit/implicit time scheme
  - High order accurate hybrid explicit/implicit time scheme
  - High order explicit local time step strategies
- Non-confirming multi-element DGTD formulation
  - Extention to 3D and parallelization aspects
  - *hp*-adpativity strategy
- DGDT method for complex propagation media
  - Extension to Drude and Drude-Lorentz models
  - Validation and assessment through collaborations with physicists

Closure

Thank you for your attention!

- Particular thanks to:
  - Tristan Cabel (Temasek Laboratories, National University of Singapore, formerly INRIA, NACHOS project-team)
  - Stéphane Descombes (University of Nice-Sophia Antipolis and INRIA, NACHOS project-team)
  - Clément Durochat (PhD student, INRIA, NACHOS project-team)
  - Loula Fezoui (INRIA, NACHOS project-team)
  - Maciej Klemm (Centre for Communications Research, Department of Electrical and Electric Engineering University of Bristol)
  - Ludovic Moya (PhD student, INRIA, NACHOS project-team)
  - Claire Scheid (University of Nice-Sophia Antipolis and INRIA, NACHOS project-team)